The Dissertation Committee for Elaine Louise Ellerton Certifies that this is the approved version of the following dissertation:

ZINC-FINGER TRANSCRIPTION FACTORS AND THE RESPONSE OF NON-MYELINATING SCHWANN CELLS TO AXONAL INJURY

Committee:

_____

Mendell Rimer, Supervisor

_____

Wesley J. Thompson, Co-supervisor

_____

Nigel Atkinson

_____

Harold Zakon

_____

Ted Mills

ZINC-FINGER TRANSCRIPTION FACTORS AND THE RESPONSE OF NON-MYELINATING SCHWANN CELLS TO AXONAL INJURY

by

Elaine Louise Ellerton, B.S.; M.S.

Dissertation

Presented to the Faculty of the Graduate School of

The University of Texas at Austin

in Partial Fulfillment

of the Requirements

for the Degree of

Doctor of Philosophy

The University of Texas at Austin

May 2008

Dedication

This is dedicated to all of my grandparents with whom I was lucky enough to spend so much time. I especially wish to acknowledge my grandfather, Sydney, whose love of science was passed down to me.

Acknowledgements

I would like to thank my mentor, Dr. Mendell Rimer, for his guidance and support over the past five years. I am also very thankful for the patience and encouragement of my wonderful committee members.

I also want to thank previous members of my lab, Vita Vock and Olga Ponomareva. I couldn't have done it without either of you.

Finally, I would like to thank my soon-to be-husband, CJ, my mother, Anneliese and my brother, Shôn, for their support. Last, but not least, I'd like to thank my dog, Carmen, and my cat, Oi, who have always stood behind me one hundred percent.

Zinc-finger transcription factors and the response of non-myelinating Schwann cells to axonal injury

Elaine Louise Ellerton, Ph.D.

The University of Texas at Austin, 2008

Supervisors: Mendell Rimer and Wesley Thompson

Schwann cell (SCs) are the glia of the peripheral nervous system. During development, a common precursor develops into two distinct types of SCs: myelinating SCs and non-myelinating SCs. There is little literature regarding the non-myelinating variety of SCs, specifically a type of non-myelinating SC found at the neuromuscular junction (NMJ), the terminal Schwann cell (tSC). Terminal SCs are critical for the maintenance and recovery of the NMJ. Peripheral nerve injury causes tSCs to become reactive, a state characterized by changes in gene expression and the extension of cellular processes. It is in this state, that tSCs help to restore functionality to the denervated junction. What drives tSCs to become reactive after injury remains largely unknown. Previously, nine zinc-finger proteins (ZFPs), a class of transcription factors, have been implicated in SC development and differentiation. As a result, transcription factors from the ZFP family were considered as potential candidates that may drive the activation of tSCs. Because tSCs are few and far between, only two-six cells cover the NMJ, I used a largely non-myelinated nerve of the autonomic system, the cervical sympathetic trunk

(CST), to search for ZFP candidates. I created a cDNA library from both control and denervated CST resulting in 40 unique ZFPs. Six of these genes were studied futher: Zipro1, Zfp36, Zfp612, Zfp180, Zfp111 and Zfp629. I found a near two-fold increase in Zipro1 mRNA and protein in denervated CST, and no change in the other five ZFPs (results from Zfp629 remain inconclusive). Using an antibody against Zipro1, I located this increase of Zipro1 to the SCs of the denervated CST. I also found Zipro1 expression in tSCs and an increase of 19% in tSCs of denervated rat muscle. Upregulation of Zipro1 in non-myelinating SCs suggests that Zipro1 may have a role in the activation of tSCs. Further study is needed in order to clarify the extent of Zipro1's involvement.

Table of Contents

List of Figures

List of tables

Abbreviations

CST	cervical sympathetic trunk
GFAP	glial fibrillary acidic protein
GFP	green fluorescent protein
IGL	internal granule layer
ML	molecular layer
NMJ	neuromuscular junction
RT-PCR	reverse transcription-polymerase chain reaction
SC	Schwann cell
SCG	superior cervical ganglion
tSC	terminal Schwann cell
ZFP	zinc-finger protein
Zipro1	zinc proliferation 1

CHAPTER 1: GENERAL INTRODUCTION

Glia- the understated cells

Glia are non-neuronal cells of the nervous system, outnumbering neurons 10 to 1. These pervasive cells have often been referred to as support cells or general care-takers, contributing little to neural function. This notion of glia is rapidly changing as these cells are redefined as active partners to neurons in the nervous system and not just as innocent bystanders. There are two major classes of glia: microglia and macroglia. Microglia are a type of macrophage, an immune cell that engulfs and destroys pathogens and intruders, thus protecting neurons in the central nervous system. Macroglia consist of four types of cells in the central nervous system: astrocytes, oligodendrocytes, ependymal cells, and radial glia. Macroglia of the peripheral nervous system consists of one type of cell, the Schwann cell (SC). Schwann cells of the peripheral nervous system appear to perform many similar functions as astrocytes and oligodendrocytes of the central nervous system. Therefore, it is likely that the study of SCs will have implications for how both these types of glia behave and function in the central nervous system.

Schwann Cells

Schwann cells (SCs), the glia of the peripheral nervous system, arise from the neural crest during development. A common precursor cell results in two types of SCs, myelinating and non-myelinating SCs. Myelinating SCs wrap around axons and form myelin, a lipid-rich substance that serves as an insulating coat. Myelin allows an electrical current to propagate down an axon with little attenuation, thus preserving the

integrity of this signal. The production and or maintenance of the myelin sheath have many clinical implications because many motor system disorders, such as multiple sclerosis, stem from the dysfunction of this sheath. As a result of the high number of myelin related disorders, most research has focused on myelinating SCs and little is known about their non-myelinating cousins.

Non-myelinating SCs are normally associated with small caliber, sensory axons, such as c-fibers, and are also associated with pre-synaptic axon terminals at a particular peripheral synapse, the neuromuscular junction (NMJ). The glial cells that reside at the NMJ are known as terminal SCs (tSCs). After peripheral nerve injury, both myelinating and non-myelinating SCs play extremely important roles during the regeneration of the axon at the NMJ. Both SCs and tSCs produce and release a number of crucial molecules such as neurotrophic factors, cell-adhesion molecules (Levi et al., 1995) and cytokines (Jander et al., 2002) that aid in the reinnervation of the synapse.

Schwann cells express different genes after denervation

In vivo, nerve injury triggers a process known as Wallerian degeneration. During this process damaged axons and their associated myelin begin to degenerate and become phagocytosed by SCs and macrophages distal to the site of injury. This process is necessary in order for the synapse to begin the regeneration process (Fawcett and Keynes, 1990). After nerve injury, SCs de-differentiate, or become 'reactive', reverting to an earlier developmental stage. These reactive SCs begin to express a different pattern of genes. For example, changes in gene expression induce the production of the low affinity NGF receptor. This receptor is not expressed in adult SCs but is rapidly upregulated in SCs found in the distal stump of the axotimized nerve 36 hours post nerve injury (You et al., 1997). Neuregulins and their receptors erbB2 and erbB3, are also upregulated in SCs

after denervation (Carroll et al., 1997). Similarly, nestin, a type VI intermediate filament protein, is also normally absent in a particular type of SC, the terminal SC, but becomes abundant 3 days after axotomy (Kang et al., 2007). Changes in gene expression, along with the release of mitogens and cytokines, enable the SCs to proliferate and speed up neuronal regeneration that aid in the demyelination, phagocytosis and regeneration of the axon (Carroll et al., 1997). Which molecules are responsible for changes in gene expression after injury are still unknown, but this change in gene patterning is crucial in order for reinnervation of the junction to occur.

Terminal Schwann cells

Terminal SCs (tSCs) are non-myelinating SCs that make up one component of the tripartite NMJ. The other two components of the NMJ are the motor axon, and the underlying muscle fiber. Terminal SCs cap the motor axon terminal, that resides directly above the post-synaptic muscle membrane. A synaptic cleft separates the two sides. Terminal SCs do not just support the NMJ, as was once thought. Terminal SCs play critical roles that extend beyond that of support for this tripartite synapse (Auld and Robitaille, 2003; Kang et al., 2003). Known roles for tSCs include the function, maintenance, formation and plasticity of the synapse (Araque et al., 1999), although new roles for tSCs continue to be discovered.

Roles of terminal Schwann cells

Terminal SCs can modulate synaptic transmission

Terminal SCs express many different types of membrane bound receptors and ion channels. Although tSCs do not have the ability to fire action potentials, they can alter synaptic transmission by eavesdropping on neuronal activity through these receptors. For

example, in the frog, stimulation of the nerve terminal at the NMJ creates an increase in intracellular calcium levels in tSCs (Jahromi et al., 1992). Receptors on tSCs appear to be responsible for this increase in intracellular calcium as blockage of neurotransmission from the nerve terminal prevents this increase (Robitaille et al., 1997). By monitoring activity at the synapse, tSCs are able to directly modulate synaptic transmission. Binding of neurotransmitters and other molecules to G-protein coupled receptors on tSCs initiates a G-protein mediated pathway that results in a decrease in neurotransmitter release from the pre-synaptic cell. This is thought to occur through the release of nitric oxide from the tSC (Robitaille, 1998). Blocking receptors on tSCs, thus inhibiting the G-protein pathway, no longer caused a decrease in the amount of transmitter released from the pre-synaptic cell (Robitaille, 1998). Terminal SCs also have a role in buffering excess potassium ions, resulting from an increase of neuronal activity, at the NMJ. This buffering of potassium may be due to the tSC's cells ability to reposition potassium channels on their membranes allowing for the removal of potassium from areas of high concentration (Kang et al., 2003).

Terminal SCs role in NMJ maintenance

Another role for tSCs at the NMJ is in the maintenance of the synapse. Ablation of tSCs at the adult frog NMJ has no initial effect on the survival or morphology of the junction. However, these synapses cannot be maintained and after one week the axons begin to retract resulting in denervation of the junction (Reddy et al., 2003). The same results have also been shown in transgenic mice that lack all SCs. The lack of SCs, including tSCs, is created by knocking out receptors for neuregulin, a growth factor that is necessary for the survival of SCs in the mouse. NMJs are formed but soon thereafter begin to disassemble, leading to extensive motorneuronal death (Lin et al., 2000).

Together, these experiments indicate that SCs are not necessary for synaptogenesis per se, but are required for the maintenance of the NMJ.

Terminal Schwann cells and the reinnervation process

Axonal injury creates a change in the pattern of gene expression in tSCs and also results in a change of morphology. Under normal conditions, tSCs have short processes, or projections, that extend from the cell. These extensions cover the nerve terminal at the NMJ. In 1992, Reynolds and Woolf showed that after denervation these tSC processes begin to extend away from the denervated junction, forming an elaborate network that reaches several hundred micrometers in length. After reinnervation of the junction, these processes retract.

The function of these extended tSC processes was elucidated in 1995 by Son and Thompson. It was already known that SCs were excellent substrates for axonal growth in vitro (Bixby et al., 1988), but it was not known whether this was true in vivo. Son and Thompson were able to visualize this process in vivo using antibodies to label axons and reactive SCs in the denervated junction of the adult rat soleus muscle. Using fluorescent microscopy they took images that showed regenerating axons following pre-existing, axonless nerve sheaths, left over from previous axons, back towards denervated endplates. Once these axons reached the endplate, some fibers continued on and grew into the muscle. These escaped fibers followed tSC processes from other junctions that had extended and formed bridges from one endplate to another (Fig 1.1) (Son et al., 1996)

Fig 1.1 Terminal Schwann cells processes form bridges linking denervated and innervated junctions.

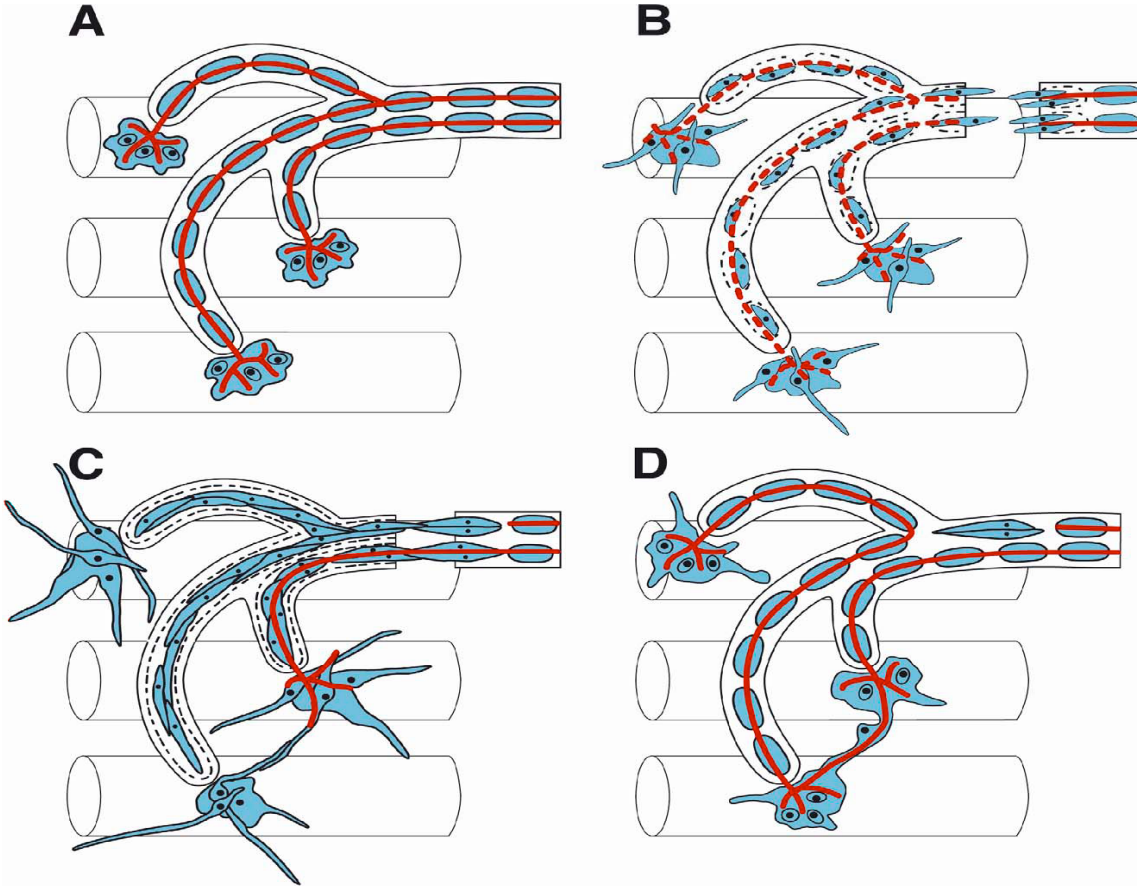

Fig1.1.Terminal Schwann cells processes form bridges linking denervated and innervated junctions: (A) Depicts an axon innervating 3 separate muscle fibers. (B) Depicts transection of the axon and the beginning of SC process extension (in blue). (C) Depicts reinnervation of one NMJ from an axon (in red) following the old nerve sheath and resulting in terminal sprouts that follow individual TSC process. TSC processes have formed a bridge linking the denervated junction to the innervated junction. (D) Depicts the reinnervation of the bottom NMJ from the axon crossing the SC bridge and then retrogradely growing up the old nerve sheath and then innervating the top NMJ. (Modified from Son, Trachtenberg, & Thompson, 1996).

These images from Son and Thompson supported the idea that axons did have a

preference for growing along tSC processes in vivo, but what remained unclear was whether the tSC was guiding the axon or whether the axon was guiding the tSC process. This was difficult to interpret with static pictures. In 2003, Kang and colleagues designed a double transgenic mouse in which all components of the NMJ could be observed using fluorescent microscopy. In this mouse, green fluorescent protein (GFP) was downstream from regulatory sequences for S100, a SC specific marker, and cyan fluorescent protein (CFP) was downstream of regulatory sequences for Thy-1, a neuronal-specific marker. In this mouse, SCs were labeled with GFP, axons with CFP, and acetycholine receptors were labeled with a non-saturating amount of rhodamine-conjugated bungarotoxin (Fig 1.2) (Kang et al., 2003). Using in vivo imaging, they showed conclusively that the axons were indeed guided by the tSC processes and not the other way around.

Fig 1.2 In vivo reinnervation of two neuromuscular junctions in the murine soleus muscle.

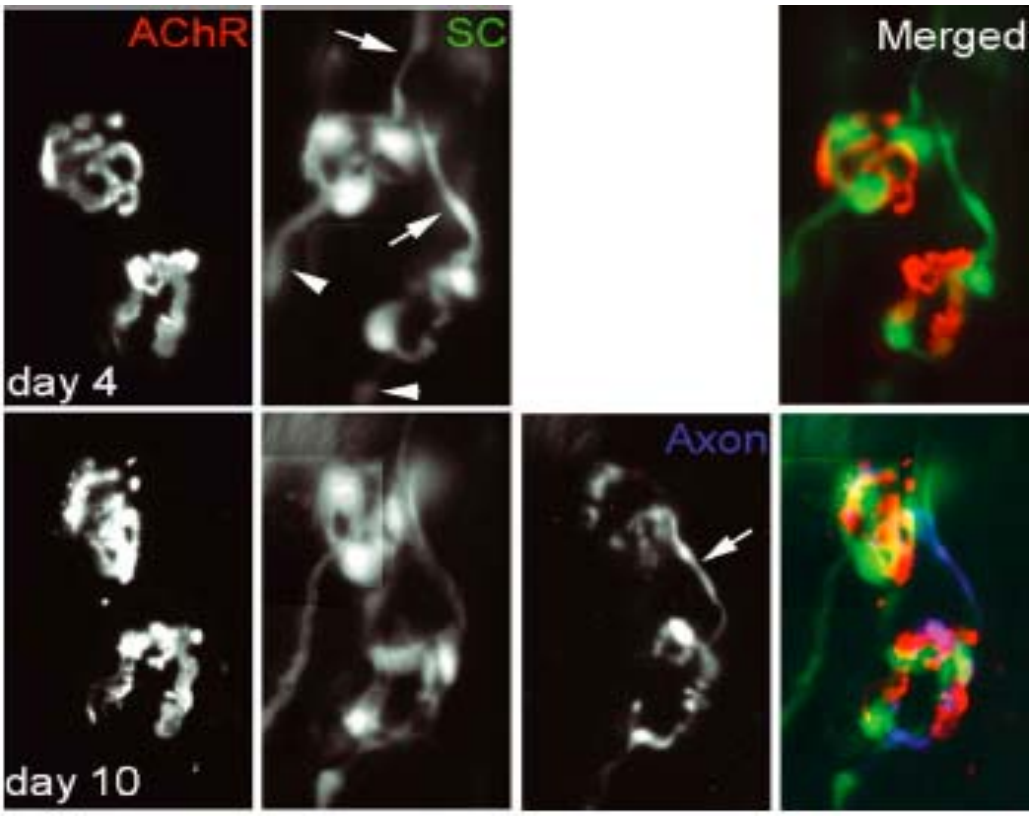

Fig 1.2. In vivo reinnervation of two neuromuscular junctions in the murine soleus muscle. The top three panels show degeneration of the nerve after 4 days. Acetycholine receptors (AChR) are stained with rhodamine-bungarotoxin and show the former synaptic site without the presence of the axon. Schwann cells (SCs) have extended processes (arrows), one which has grown from the lower synaptic site in the direction of the upper synaptic site. Arrowheads depict the old endoneurial tube. There is no CFP-labeled axon panel at this point. After day 10 of denervation, the old synaptic sites mostly retain their shape (AChR). A CFP-labeled axon has sprouted from the lower junction and has followed the old endoneurial tube up and reinnervated the upper junction. (Modified from Kang et al., 2003).

In summary, tSCs have more roles at the NMJ then a supporting one. Their roles in the plasticity and maintenance of the NMJ are critical for synaptic function. Specifically, their role in the reformation and recovery of the synapse after injury is of clinical importance.

Zinc-finger protein transcription factors in SC development

Most zinc-finger proteins (ZFPs) are transcription factors, proteins that regulate and control the conversion of genetic information from DNA into RNA. The ZFP family constitutes the largest family of transcription factors (Klug, 2005). Zinc-finger proteins interact with DNA through their highly conserved zinc-finger domains. Each domain consists of two antiparallel β sheets, an α helix, and a stabilizing zinc ion. The specific residues that make up the α helical portion of the zinc-finger determine the binding specificity. The amino acid sequence encoding each finger is highly conserved and consists of about thirty amino acids. The conserved consensus sequence for an individual finger is Cys-X2-4-Cys-X3-Phe-X5-Leu-X2-His-X3-His. The structure is shown in fig 1.3.

Fig 1.3 A cartoon representation of a zinc-finger protein motif.

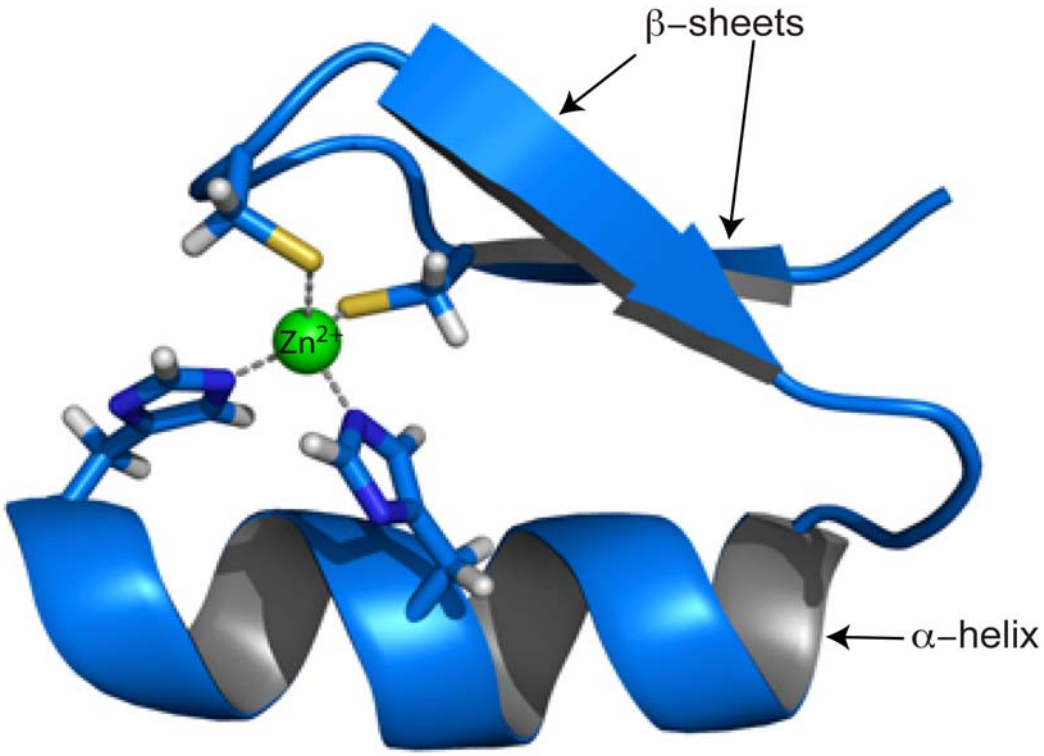

Fig 1.3 A cartoon representation of a zinc-finger protein motif. The structure consists of an α helix and two antiparallel β sheets. A zinc ion (green) is crucial for the molecule's stability. Figure was modified from original obtained from Wikipedia, author Thomas Splettstoesser.

The development of neural crest cells into SCs, and the decision concerning whether or not they will have the ability to produce myelin, is dependent on certain transcription factors (Jessen and Mirsky, 2002). At lease nine ZFPs have been identified in SCs and are implicated in their development. Several of these are from a family of immediate-early genes, the early growth response (Egr) family, and some are responsible for changes in gene expression after injury. For example, *Egr2* (*Krox20*) is essential in

determining whether a precursor SC will become a myelinating or a non-myelinating SC (Topilko et al., 1994; Jessen and Mirsky, 2002), while *Erg1* (*Krox24*) is expressed and upregulated in SCs, after nerve injury (Topilko et al., 1997). Because of the pre-existing evidence of ZFP involvement in transcriptional changes in SCs, it is likely that this class of transcription factor has implications for the reactivation of tSCs after injury.

Cervical sympathetic trunk

Studying tSCS is a difficult endeavor. One reason for this difficulty is the lack of a specific marker for tSCs. Both myelinating SCs and non-myelinating tSCs arise from a common precursor; therefore they express many of the same genes. For instance, S100 is a marker for tSCs, however it labels all types of SCs. Neuregulin-2 is expressed by tSCs but also by motor neurons and other interneurons in the spinal cord (Rimer et al., 2004). Other markers, such as protein zero (P0) and myelin-associated glycoprotein (MAG), are expressed in both types of SCs as well, although their expression is weaker in tSCs (Georgiou et al., 1994). Specific markers exist for tSCs in other model systems such as frogs and snakes. Lectin peanut agglutinin specifically labels tSCs in frogs and snakes (Ko and Chen, 1996), whereas a monoclonal antibody (2A12) only labels tSCs at frog NMJs (Astrow et al., 1997). No specific marker exists for mammalian tSCs yet.

Other difficulties in studying tSCs are their scarcity and their location. There are only two-six tSCs per NMJ and only one NMJ per muscle fiber. Uncovering patterns of gene expression through the isolation of RNA from individual tSCs proves to be an arduous task. The cervical sympathetic trunk (CST) is a good way to circumvent this problem. The CST is a peripheral nerve of the autonomic system. It is composed of inputs from spinal segments TI-T7, although 90% of axons emanate from T1-T3 (Rando et al., 1981). TThe CST sends its afferents to the superior cervical ganglion. What makes

the CST preparation so appealing is that it consists of bundles of mostly non-myelinated axons. These bundles are known as Remak bundles (Aguayo, 1973). Ample material from non-myelinating SCs can be obtained from RNA isolated from the CST, as non-myelinating SCs are associated with these Remak bundles. It is possible that non-myelinating SCs of the CST may not be a perfect model for tSCs. However, their common lineage implies that they most likely share a core transcriptional program.

Rationale for this study

Understanding the molecular mechanisms that underlie non-myelinating SC activation, specifically tSC reactivation, would directly benefit the area of research surrounding axonal regeneration, not only in the peripheral nervous system, but also in the central nervous system. Difficulty of isolation and a lack of markers specific to no-myelinating SCs has prompted us to resort to using a different model, the cervical sympathetic trunk. Transcription factors from the zinc-finger family have already been implicated in various aspects of SC development, therefore I looked within this family of transcription factors to find novel genes that may be behind the reactivation of tSCs after injury.

The structure of my thesis will be as follows: Chapter two contains a manuscript, which represents the majority of my findings for this dissertation. This manuscript is currently in press in Neuroscience. Chapter three contains additional data and results not included in my manuscript. Chapter four summarizes my findings and discusses future directions and conclusions of my work. Finally, chapter five provides a detailed methodology of my work.

CHAPTER 2: INDUCTION OF ZINC-FINGER PROLIFERATION 1 EXPRESSION IN NON-MYELINATING SCHWANN CELLS AFTER DENERVATION

Abstract

Terminal Schwann cells (tSCs) are non-myelinating glia that cover the nerve terminal at the neuromuscular junction. They are required for the maintenance of the neuromuscular synapse and are likely to play essential roles in the restoration of synaptic connections after nerve injury. Terminal SCs acquire a reactive phenotype after nerve damage characterized by the extension of cellular processes that may facilitate reinnervation. The molecular signaling events underpinning the tSC reactive state remain elusive, in particular, little is known about transcription factors involved in the transcriptional reprogramming during tSC activation. Prior research implicated nine members of the zinc-finger transcription factor family in SC development and myelination, and levels of one such protein were reported increased in other nonmyelinating SCs after denervation. We hypothesize that zinc-finger transcription factors could play a role during tSC activation. Because of their relative paucity, tSCs are difficult to study molecularly. Here, we used the rat cervical sympathetic trunk (CST), an autonomic nerve in which non-myelinating SCs are the predominant cell type, to isolate zinc-finger protein (ZFP) cDNAs by RT-PCR. We isolated 29 unique ZFP sequences of which zinc proliferation 1 (Zipro1) was the most abundant. We found that after CST transection, levels for Zipro1 mRNA doubled and that Zipro1 protein expression increased in non-myelinating CST SCs. We also determined that Zipro 1 is expressed in tSCs and its levels increased following skeletal muscle denervation. Thus, Zipro1 is a

good candidate for a transcription factor involved in activation of non-myelinating SCs in general, and tSCs in particular.

Introduction

Schwann cells (SCs) are the glia of the peripheral nervous system. During development, the neural crest gives rise to two distinct types of SCs, one that produces myelin and one that does not (Jessen and Mirsky, 2002). Given their importance in myelin generation, and perhaps because of the associated human demyelinating neuropathies, much of the work on SCs has focused on the myelinating cells, whereas much less is known about the non-myelinating SCs. Specifically, little is known about a type of non-myelinating SC at the neuromuscular junction (NMJ), the terminal Schwann cell (tSC). These cells are required for NMJ maintenance (Reddy et al., 2003). In addition, tSCs likely play an essential role in re-establishment of synaptic connections following nerve injury in adult animals (Kang et al., 2003). Denervation induces dramatic changes in tSC gene expression and morphology. These "reactive" tSCs change their gene expression (Kang et al., 2007) and generate de novo cellular processes, which provide a favorable substrate for the incoming nerve to reform connections at the original synaptic sites during regeneration. The molecular mechanisms underlying the tSC reactive state remain elusive largely because of the paucity of specific molecular markers associated with this process. In particular, little is known about transcription factors that may be involved in the transcriptional reprogramming that takes place upon tSC activation.

The zinc-finger protein (ZFP) family is the largest family of transcription factors

in the mammalian genome (Klug, 2005). Previous research has implicated at least nine members of this family in SC development and myelination (Alonso et al., 2004). One zinc-finger transcription factor in particular, Egr-1 (also known as Krox24), was found upregulated in non-myelinating SCs after denervation (Topilko et al., 1997). Thus, it is reasonable to hypothesize that transcription factors belonging to this family could also be involved in the phenotypic changes during tSC activation. Terminal SCs are difficult to study biochemically as their numbers per muscle are very low. There are only 2-6 tSCs per NMJ, one NMJ per muscle fiber. Most relevant in this context is the fact that a NMJ represents only 0.1% of the muscle surface. Hence, once a muscle is homogenized, the fraction of tSC-specific RNAs and/or proteins is very low. One way to circumvent this limitation is to use a preparation in which non-myelinating SCs, similar to tSCs, represent the predominant cell type. Such a preparation is provided by the cervical sympathetic trunk (CST) (Aguayo et al., 1976), an unmyelinated preganglionic trunk of the superior cervical ganglion.

Here, we used degenerate primers to the conserved C_2H_2 motif in zinc-finger transcription factors to isolate ZFPs cDNAs from the CST in the adult rat by RT-PCR. We generated a library of partial cDNAs encoding 29 unique ZFPs. The cDNA for zinc-finger proliferation 1 (Zipro1, also known as RU49, ZFP38) (Chowdhury et al., 1992);(Yang et al., 1996) was the most abundant sequence in our library. Thus, we next studied the expression and regulation by innervation of Zipro1 in the CST. We found that Zipro1 mRNA was increased after denervation of the CST. This increase appeared selective as mRNA levels for another gene highly represented in our library, zinc finger protein 36 (Zfp36) was unchanged. Using a previously uncharacterized, commercial antibody against Zipro1, we found by Western blot analysis that Zipro1 protein was also

increased after CST denervation. Immunocytochemical staining with the same antibody showed that Zipro1 is present in SCs and neurons in the CST, but that the increase in protein levels after denervation was limited to the SCs and not the neurons. Lastly, tSCs stained for Zipro1 and also showed an increase of such staining after skeletal muscle denervation. Thus, Zipro1 is a good candidate for a transcription factor gene involved in activation of non-myelinating SCs in general, and tSCs in particular.

Materials and methods

Animal Surgeries

All surgical procedures and animal care followed institutional and NIH guidelines. For CST: adult male and female Sprague-Dawley rats (95-215 g) were anesthetized by intraperitoneal injection of Nembutol® Sodium Solution (62 mg/kg). A ventral mid-cervical incision was made and the cervical sympathetic trunk (CST) was transected at a distance of 2–3 cm caudal to the superior cervical ganglion (SCG). Following surgery, animals were allowed to recover for 3 or 4 days. Successful surgeries were demonstrated by ipsilateral ptosis. Animals were then sacrificed by CO2 inhalation and both denervated and intact CSTs were harvested and frozen in liquid N_2. The segment of the transected CST removed for analysis was between the lesion and the SCG. For muscle: murine leg muscles were denervated by cutting the sciatic nerve under anesthesia. An injection of a 75 mg/ml ketamine, 5 mg/ml xylazine mixture was administered i.p. for every 100 g in weight. Animals were sacrificed 3–4 days after denervation, and muscles were removed and processed as described below.

Tissue culture and transfection

The SC line D6P2T (Bansal and Pfieffer 1987) and the human embryonic carcinoma 293T cells were grown in DMEM with 10% FBS and 50 μg/ml gentamycin.

Reverse transcriptase-polymerase chain reaction (RT-PCR) and Isolation of a Zinc Finger Motif-enriched cDNA Library

CSTs were harvested as above. Total RNA was prepared with RNA STAT-60 reagent according to the manufacturer's instructions (Tel-Test, Friendswood, TX). SuperScript II reverse transcriptase (Invitrogen, Carlsbad, CA) was used to make cDNA from 500 ng of RNA per sample, and 1/10th of the reaction was used for PCR with HotStart PCR Master Mix (Qiagen, San Diego, CA). The following degenerate primers were used for isolation of ZFPs: CysX2 5' -TGCCCNGAGTGYGGNAAR-3' and H/C 5' -NGGCTTCTCNCCNGTATG-3'. Cycling parameters were 15 min at 95°C, 1 initial cycle for 3 min at 94 °C, followed by 40 cycles for 1 min at 94 °C, 1 min at 48 °C and 1 min at 72 °C, and a final extension for 10 min at 72 °C. (Alonso et al., 2004). Samples were run in 2% agarose gels. Amplified bands were isolated using Qiaex (Qiagen, San Diego, CA) and directly subcloned into the pCR2.1-vector (TA cloning kit, Invitrogen, Carlsbad, CA) to generate a zinc finger motif enriched cDNA library. Individual clones were randomly selected and their identity was confirmed by DNA sequencing.

Semi-quantitative PCR

Semi-quantitative PCR was done by collecting aliquots from PCR reactions at different cycles during amplification. The collected samples were run on a 1% agarose

gel containing ethidium bromide and an image was captured. Average grey values of the bands were quantified using Metamorph 5.0 (Universal Imaging). The results were graphed with the log of average grey values vs. linear cycle numbers. Differences in mRNA values were obtained using linear regression from equations obtained from lines fit to the data points. Primer sequences were: Zipro1: Forward 5'- AGT CCC AGG TTT GGA GTG TG-3'; Reverse 5'-GAA GGT CCC AAC TGT AA-3'. Zfp36: Forward 5'-CCC TGT TGG ACT CCA CCT AA-3'; Reverse 5'-GCC TCT TCT CCA CTG TCA GG-3'. β-actin: Forward 5'-GCT ACA GCT TCA CCA CCA CA-3'; Reverse 5'-AAG GAA GGC TGG AAA AGA GC-3. Cycling parameters were 95°C for 15 min, 39 times at 94°C for 1 min, 50°C for 30 s and 72°C for 30 s, followed by a final extension at 72°C for 10 min.

Western Blotting

Cerebellum, kidney, liver, skeletal muscle, and both transected and control CSTs, were removed from rats and snap frozen in liquid N2. Cerebellum, kidney and liver were homogenized with a polytron in a ice-cold RIPA buffer with 10% v/v Protease Inhibitor cocktail (Sigma, St. Louis, MO). CSTs were homogenized by sonication in the same buffer. The extracts were passed through a 21-gauge needle several times to reduce viscosity and stored at -80°C until use. D6P2T and 293T cells were cultured as above, rinsed in cold PBS, and scraped from the dish in RIPA buffer with 10% v/v Protease Inhibitor cocktail (Sigma, St. Louis, MO); cells were broken up by passage of the suspension through a 21-gauge needle several times. Samples were spun down for 10 min at 1000g at 4°C. Supernatants were concentrated using a Centricon YM-30, 30,000 MW cut-off (Millipore Corp., Bedford, MA), following the manufacturer's instructions. Protein concentration was estimated using Bradford-based, Biorad Protein Assay (Biorad,

Hercules, CA). The indicated amount of each extract was mixed with 2x Laemmli sample buffer (Sigma, St. Louis, MO), heated for 5 min at 95°C, and fractionated in 7.5% acrylamide denaturing gels and transferred to PVDF membranes. Western blots were blocked with 5% non-fat milk in TBS-T and probed with Zipro1 antibody, used at 1/350 dilution. Horseradish Peroxidase-conjugated anti-rabbit secondary antibody (Jackson Immunoresearch, West Grove, PA) was used at 1/3000 dilution. Antibody-binding was detected by chemiluminescence according to the manufacturer's instructions (Perkin Elmer). For normalization, membranes were stripped, blocked and re-probed with a monoclonal antibody to α-tubulin (T-9026; Sigma, St. Louis, MO), used at 1/4000 dilution and Horseradish Peroxidase-conjugated anti-mouse secondary at 1/4000 (Jackson Immunoresearch, West Grove, PA). For quantification, film was scanned and images were saved as TIFF files. Optical

density measurements were taken from scans of films using MetaMorph 5.0 software (Universal Imaging). The value for denervated CST was divided by the value for the control CST for both Zipro1 and α-tubulin. For normalization, the ratio obtained for Zipro1 was then divided by the ratio for α-tubulin.

Antibodies and immunohistochemistry

Antibodies used were as follows: polyclonal antibody raised in rabbit against the peptide sequence SNLTKHRRTHTGEKPY of Zipro1 (ZFP38/RU49) (PA1-17222; Affinty BioReagents, Golden, CO) used at 1:250- 1:5000 dilution. A monoclonal antibody to SV2, used at 1:200 (Developmental Studies Hybridoma Bank, University of Iowa), and a monoclonal antibody to neurofilament (NF), used at 1:250 (2H3; Developmental Studies Hybridoma Bank, University of Iowa) was used to mark neurons. A rat anti-mouse antibody to CD68 (MCA19578; Serotec), to mark macrophages, was

used at 1:50. A polyclonal rabbit antibody to S100β (Z0311, Dako), used at 1:400, and anti-glial fibrillary acidic protein (GFAP; G3893; Sigma, St. Louis, MO) used at 1:200. Secondary antibodies included goat anti-rabbit rhodamine-conjugated secondary antibody (111-025-144, Jackson Immunoresearch, West Grove, PA) at 1:400 dilution. Fluorescein or Alexa-647 α-bungarotoxin (B-35450, Molecular Probes, Eugene, OR), used at 1:400 to mark AChRs, was added for the last 20 minutes during the 1 hr incubation period and DAPI(D-1306, Molecular Probes, Eugene,OR) was added for the last 5 min to label cell nuclei at 1:1000.

Frozen sections of unfixed CST, skeletal muscle, and brain were stained as described previously (Rimer et al. 1998). Whole mount staining was performed as follows. Soleus, gastrocnemius and tibialis muscles were removed and pinned on a Sylgaard dish with steel insect pins. They were then fixed in 4% paraformaldehyde (PFA) for 30 min, washed 3 times for 10 min in PBS, then 1 time for 10 min in PBS-T. The muscles were teased apart and then blocked for 30 min in blocking solution (0.5% Triton-X100, 2% BSA in PBS). They were then incubated with primary antibody in blocking solution overnight at room temp. The next day they were washed 3 times for 20 min in blocking solution then incubated in secondary antibody for 1 hr at room temp. Junctional regions were visualized with fluorescein- or Alexa-647- α-bungarotoxin in blocking solution for 45 min to mark AChRs. DAPI was added in the last 5 min of staining to label cell nuclei. They were then washed 3 times 20 min in blocking solution, overnight at 4°C in PBS-T and then stored in PBS. For quantification we used a 1:5000 dilution of the Zipro1 antibody and with Metamorph 5.0 (Universal Imaging) imaging software we measured average grey values of labeled cells. Values were averaged for cells from both control and denervated tissues and a two-tailed t-test was used to determine statistical

significance.

In situ hybridization

A Zipro1 probe was prepared from primers consisting of a clamp sequence, a core promoter and the gene specific sequence. For the antisense probe the clamp sequence was 5'- CAGAGATGCA-3', a T3 core promoter 5'- ATTAACCCTCACTAAAGGGAGA-3' and gene specific sequence of 5' -CCTTCGCCCATTAAAGTTGA-3'. For the sense strand, clamp region was 5' -CCAAGCCTTC-3', T7 promoter 5'-TAATACGACTCACTATAGGGAGA-3' and gene specific sequence 5'-TTTTGAGTCCACCTGCATGA-3'. Amplification parameters were: 95°C for 15 min, 3 times at 94°C, 52°C for 2 min, and 72°C for 1.5min, 36 times at 94°C for 1 min, 62°C for 1 min and 72°C for 1.5 min followed by a final extension of 72°C for 5 min). The probe was labeled with digoxigenin (Rimer et al. 2004) and chemically hydrolyzed (Schaeren-Wiemers and Gerfin-Moser 1993). Rat CST and Cb were removed and snap frozen in liquid N2. In situ hybridization was performed on 12 μm cross sections following a protocol from (Braissant and Wahli 1998) with some modifications. Hybridization was carried out at 52°C for 48 hours. One hour wash in 2 x SSC was carried out at 61°C.

Results

Isolating cDNAs for zinc finger proteins (ZFPs) in CST

Zinc-finger transcription factors share a highly conserved C2H2 motif with a consensus sequence (Tyr/Phe)-X-Cys-Xm-Cys-X3-Phe-X5-Leu-X2-His-Xo-His-Xn (m is 2 or 4; n is often 5; o is 3 or 4; X is a variable amino acid). This zinc-finger motif

consists of around 23 amino acids with about 7-8 amino acids linking each finger (Alonso et al., 2004). Degenerate primers were designed from this highly conserved sequence (Alonso et al., 2004) and were used to amplify ZFPs in cDNA prepared from total RNA isolated from CST. This product was then run on an agarose gel revealing a ladder of bands, where each band is represented by partial ZFP sequences containing a certain number of C2H2 zinc-finger motifs. We cut five of the bands, representing sequences with 2-6 zinc-finger motifs, from the gel and subcloned the purified DNA. We selected a total of 60 colonies for sequencing, and using data base analysis, we compared our sequences against known sequences resulting in a library containing 29 unique ZFP genes, many uncharacterized. All of the clones contained a zinc-finger motif and lacked intronic sequences. A complete list of these genes is given in table 1. We failed to detect sequences for *Egr-1*. Out of the 60 colonies sequenced, several genes appeared multiple times. These included *Zfp36*, which occurred 3 times, and *zinc-finger proliferation 1* (*Zipro1*), which occurred 8 times. As non-myelinating Schwann cells are the predominant cell type in the CST (Aguayo et al., 1976), we reasoned that these most abundant sequences in our library were most likely expressed by these cells. Thus, this prompted us to study them further.

Table1:Zinc-finger library prepared from control adult rat CST

Table 1. Zinc-finger library prepared from adult rat CST

Insert	Colonies sequenced	Homolog to (Accession #)	Gene name (and other names in literature)	Reported expression in glial cells?	References
1	8	NM_001012021	Zipro1 (Ru49, Zfp38)	No; cerebellum, skin, and testes	1, 20
2	3	NM_001025760	Zfp36 (KOX 18, ZNF 139)	No; encodes for tristetraprolin in fibroblasts	2
3	3	NM_011762	Zfp 59	No; detected in mature sperm	3
4	3	BC079015	ZNF 61	No; detected in testis cDNA library	4
5	4	NM_133323.	Zfp111	Oligodendrocytes	5
6	1	NM_144757	Zfp180 (rKr1)	Oligodendrocytes (and neurons)	6
7	4	XM_574381	ZFP235	?	-
8	2	XM_573110	ZNF 286 (KIAA1874)	?	-
9	3	XM_577778	ZNF 545 (Zinc finger protein 30 homolog)	?	-
10	4	XM_226455	Zfp612	No; predominantly kidney	7
11	3	XM_235625	ZNF 641 (FLJ31295)	No; cancer cell lines	8
12	1	NM_001014158.	3110052M02Rik protein (similar to KRAZ1)	?	9
13	1	XM_577757	MkIAA1431protein (Mouse Zinc-finger)	?	-
14	1	XM_574405	Zfp354A (RIKEN cDNA C030039L03 gene, mouse)	No; predominantly kidney and eye	10
15	1	NM_023988.	znf 354c	No; bone	11
16	1	XM_344876	Zfp74(KRAB8, Zfp66)	No; cardiomyocytes	12
17	1	BC040201	Zfp715	Ubiquitous	13
18	1	BC082594	Zfp449	No	14
19	1	XM_574417	Zfp569	?	-
20	1	AK143471	Zfp30 (KOX28)	Ubiquitous	15
21	2	BC079105	Zfp426	?	16
22	1	U27186	Cys2/His2 zinc finger protein (rKr2)	Oligodendrocytes	17
23	2	NM_001033355	Zfp568	?	18
24	2	NM_027264	Zfp715	?	19
25	1	XM_898030	RIKEN cDNA 5730601F06	?	-
26	2	XM_576489	Zfp660	?	-
27	1	XM_577790	RIKEN cDNA 2610020C11	?	-
28	1	XM_221920	Rattus norvegicus similar to RB-associated KRAB	?	-
29	1	XM_345851	Zfp251	?	-
	60				

References

1 Nat Genet. 22(4):327-35 (1999)
2 Proc. Natl. Acad. Sci. U.S.A. 99 (26), 16899-16903 (2002)
3 Cell Growth Differ. 6 (8), 1037-1044 (1995)
4 Proc. Natl. Acad. Sci. U.S.A. 99 (26), 16899-16903 (2002)
5 J. Neurochem. 65 (5), 1955-1966 (1995)
6 Brain Res. Mol. Brain Res. 38 (1), 109-121 (1996)
7 PNAS 98(5):2199-2204 (2000)
8 Nature Genetics 24: 227-34 (2001)
9 Proc. Natl. Acad. Sci. U.S.A. 99 (26), 16899-16903 (2002)
10 Exp. Eye Res. 64 (2), 287-290 (1997)
11 J. Biol. Chem. 276 (21), 18282-18289 (2001)
12 Science 309:1564-1566(2005).
13 Proc. Natl. Acad. Sci. U.S.A. 99 (26), 16899-16903 (2002)
14 Proc. Natl. Acad. Sci. U.S.A. 99 (26), 16899-16903 (2002)
15 New Biol. 2:363-374(1990); Science 309 (5740), 1564-1566 (2005)
16 Proc. Natl. Acad. Sci. U.S.A. 99 (26), 16899-16903 (2002)
17 J. Neurochem. 65 (5), 1955-1966 (1995)
18 Genome Res. 11 (9), 1553-1558 (2001)
19 Gene 213 (1-2), 55-64 (1998)
20 Mech. Dev. 39 (3):129-42. (1992)

Zipro1 mRNA selectively increased after denervation of the CST

We sought to determine whether *Zfp36* and/or *Zipro1* expression was altered by denervation. We transected the CST unilaterally, just caudal to the SCG, in adult rats and then after 3 days removed the nerves from both the denervated and contralateral side. The denervated and control nerves were pooled separately. Total RNA was isolated from these pools and RT-PCR was performed to generate cDNA. We designed primers for *Zfp36* and *Zipro1* to look for differential expression in control and denervated CST cDNA. For PCR quantification, we first amplified *Zfp36* and *Zipro1* in both normal and denervated CST using as template 3 separate dilutions of cDNA (1/5, 1/25, 1/625) in an end-point PCR reaction. There was no difference in band intensity at the highest dilution in both control and denervated CST for *Zfp36*, whereas for *Zipro1* the highest dilution in the denervated sample showed a much more intense band (Fig 2.1A). At this dilution, it was more likely that the end-point PCR reaction reflected true differences in initial RNA levels between the samples. To quantify the difference in mRNA levels more precisely, we used semi-quantitative PCR where aliquots of DNA were removed at specific cycle numbers during the linear phase of amplification. A house keeping gene, *β-actin*, was also run at the same time for normalization purposes. The collected samples were run on an agarose gel and an image was captured allowing us to measure the average grey values of the bands. Quantification was done using Metamorph imaging software and the results were graphed with the log of average grey values vs. linear cycle numbers. Using linear regression from equations obtained from lines fit to the data points, we were able to compare differences in mRNA levels between control and denervated CST for *Zfp36,*

Zipro1 and *β-actin* (Fig 2.1B-D). After normalizing to *β-actin*, nearly a two-fold increase was seen for *Zipro1* in denervated CST relative to control (Fig 2.1E). No difference was seen in *Zfp36*. Thus, *Zipro1* expression is selectively stimulated in denervated CST.

Fig 2.1 Semi-quantitative PCR shows selective induction of *Zipro1* mRNA in denervated CST.

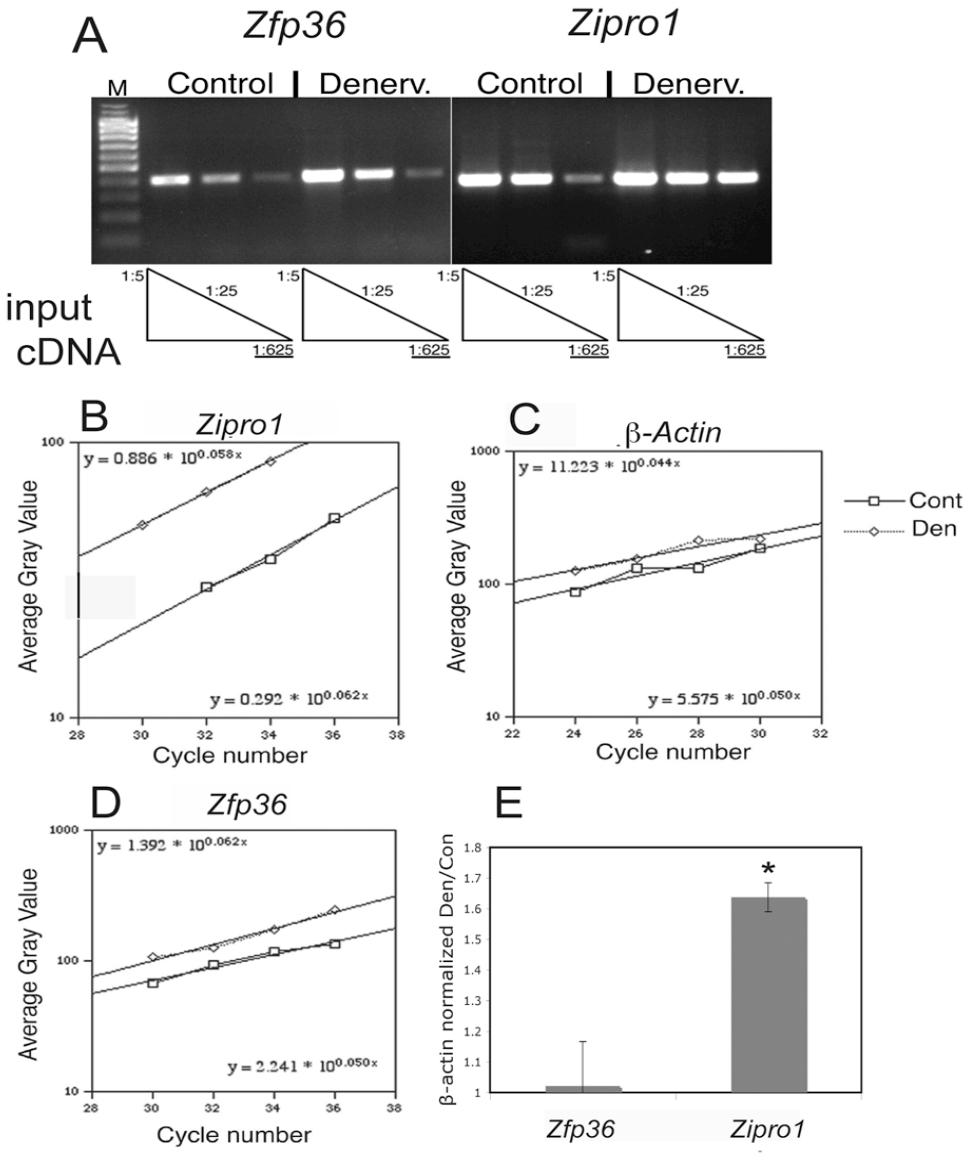

Figure 2.1. Semi-quantitative PCR shows selective induction of *Zipro1* mRNA in denervated CST. (A) Total RNA was prepared from 3-day denervated CST and contralateral control. One microgram of each sample was reverse transcribed and the resulting cDNA was diluted 1:5, 1:25 and 1:625. Endpoint PCR reactions were carried out with gene-specific primers for *Zipro1* and *Zfp36*. Amplified products were run at the same time on 2% agarose gels containing ethidium bromide. Note that at the highest dilution (1:625), where amplification is likely linear, band intensity for *Zipro1* is higher for denervated samples, while it is similar between normal and denervated samples for *Zfp36*. M: 100-bp size markers. (B-E) Semi-quantitative PCR was done by collecting aliquots from PCR reactions at different cycles during amplification. Average gray value for each band was determined and plotted vs. cycle number. Exponential fit of the data shows that amplification for each gene was in the linear range. Equations in top left of each panel correspond to denervated (Den) samples, while equations in bottom right of each panel correspond to normal (Cont) samples (B-D). To estimate expression changes, the equations were used with the following cycle number (x value): *Zipro1*, 31; *Zfp36*, 32; *β-actin*, 27. (E) Den/Cont ratios were normalized to *β-actin* values for each zinc-finger gene; n=3. * = $p < 0.05$, t-test *Zipro1* vs. *Zfp36*.

Characterization of an anti-Zipro1 antibody

We obtained a commercial antibody said to recognize the amino acid sequence SNLTKHRRTHTGEKPY of Zipro1. This sequence is outside the zinc-finger motifs. Without any published literature on the antibody, we first tested it to see if we could detect Zipro1 protein in cerebellum, a tissue previously shown to abundantly express Zipro1 by Northern blot and in situ hybridization (Yang et al., 1996). As negative control, we looked at tissues previously shown not to express Zipro1 by Northern analysis of total RNA (Yang et al., 1996). We ran a Western blot, loading equal amounts of total protein from homogenized cerebellum, liver, kidney and muscle. After probing the blot with the Zipro1 antibody, bands at the expected molecular weight of about 63 kDa were seen in all of samples. As anticipated, the band was strongest for cerebellum and much fainter for the other tissues (Fig 2.2A). A few other bands were also seen in cerebellum, one higher and two lower than Zipro1. Although the larger band, only seen in the cerebellum,

appeared too big to be encoded by Zipro1, the smaller molecular weight bands could be due to protein degradation. We also detected a moderately strong 63 kDa Zipro1 band in a human embryonic kidney cell line, 293T, and using end-point RT-PCR, we found Zipro1 mRNA in two separate mouse muscle cell lines, C2C12 and Sol8 (data not shown). Yang and colleagues (Yang et al., 1996) published in situ hybridization data showing strong expression of Zipro1 in the internal granular layer of the cerebellum and other granule cells in adult rat brain. We confirmed this finding by performing non-radioactive in situ hybridizations in the cerebellum with a probe designed against the non-zinc-finger region of Zipro1 (Fig 2.2B). However, we also detected Zipro1 mRNA staining in larger cells along the periphery of the internal granule layer (Fig 2.2D) (at the junction of the granular and molecular layers). These cells could either be Bergmann glia or Purkinje cells. We then used the commercial antibody in sagittal sections of the entire brain. Cells in the cerebellar internal granule layer were stained strongly along with the larger Bergmann or Purkinje cells in the periphery of this layer (Fig 2.2E). A population of cells was also stained in the molecular layer of the cerebellum (Fig 2.2C). These cells appeared unlabelled in the in situ experiments (Fig 2.2B). Thus, the commercial antibody appears to detect Zipro1 in both Western and immunostaining analysis. The antibody shows specificity that, by in large, matches previous reports based on mRNA analysis, and our own in situ experiments. The major discrepancy is that we detected weak Zipro1 expression in tissues and cells not expected to have it based on previous observations, such as peripheral tissues (Fig 2.2A) and molecular layer cells in the cerebellum (Fig 2.2C). It is likely that this discrepancy is explained by better sensitivity of the Western over the Northern analysis, on the one hand, and of the immunostaining over the non-radioactive in situ on the other (see also Discussion).

Fig 2.2 Zipro1 expression in cerebellum, liver, kidney, and muscle of the adult rat.

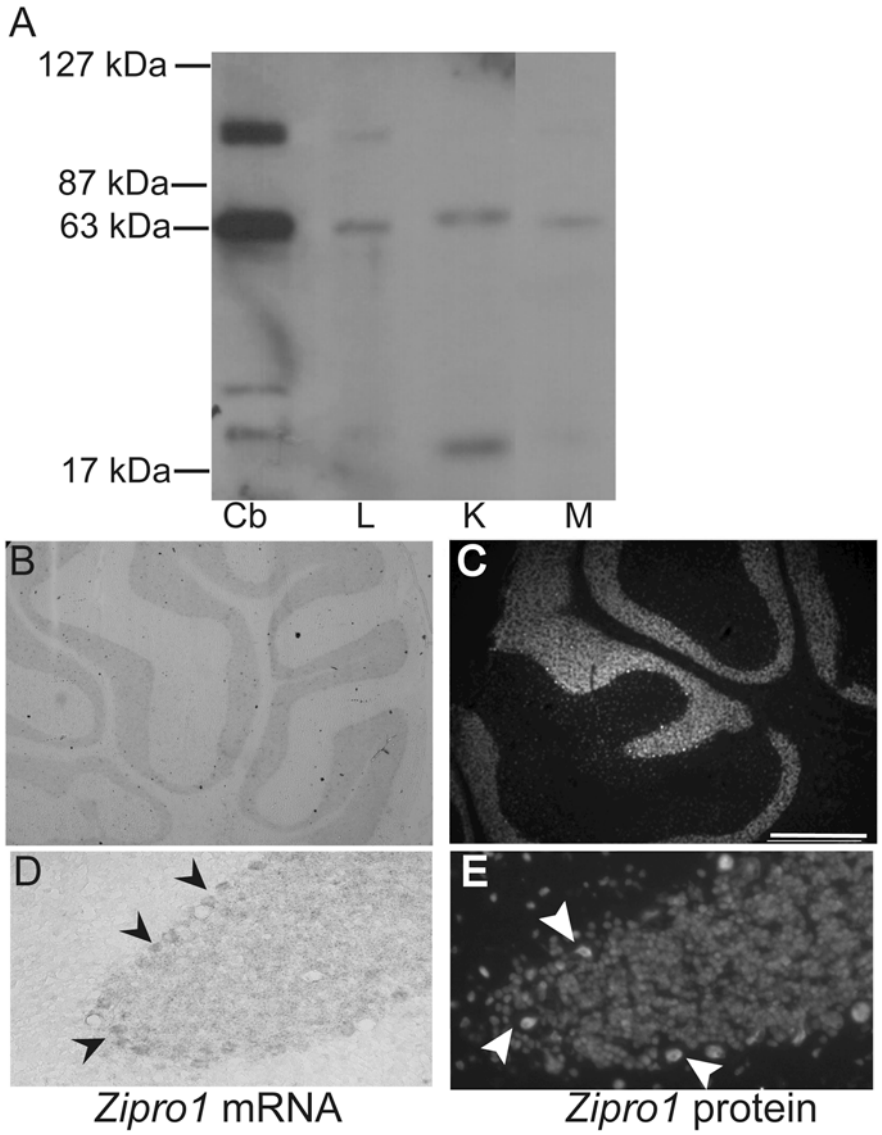

Figure 2.2. Zipro1 expression in cerebellum, liver, kidney, and muscle of the adult rat. (A) Seventy-five μgs of homogenized rat cerebellum (Cb), liver (L), kidney (K), and muscle (M) were run on a SDS-PAGE gel and transferred to a nylon membrane and probed with an antibody to Zipro1. Bands were visualized by chemiluminescence. The cerebellum (Cb) shows a strong band at the correct weight of 63 kDa, whereas weaker bands appear for L, K and M. An unknown, larger band also appears in Cb and weakly in L. Smaller bands may represent degraded proteins. (B) In situ hybridizations with an antisense non-radioactive probe against Zipro1 labels the internal granule layer (IGL) of the Cb. (Controls with sense probe were clean, data not shown). (C) Similar IGL staining of the Cb is seen with immunocytochemistry (ICC) using the Zipro1 antibody, however, cells in the molecular layer are also labeled. (D,E) At a higher magnification, in situ labeling of large cells that lie along the periphery of the IGL are seen (black arrowheads) (D). Zipro1 staining of larger cells is also evident with ICC (white arrowheads) (E). Scale bar: 150 μm.

Zipro1 protein increased after denervation of the CST

We next checked for Zipro1 protein levels in normal and denervated CST by Western blotting. We denervated CSTs unilaterally in 4 animals and removed them from 2 animals after 3 days and from 2 animals after 4 days of denervation. After normalizing to a housekeeping protein, α -tubulin, there was a 2.2 fold increase in Zipro1 protein in samples denervated for 4 days in comparison to the control (Fig 2.3). Similar results were also seen for samples obtained three days after denervation (data not shown). Thus, like Zipro1 mRNA, Zipro1 protein is also increased after CST denervation.

Fig 2.3 Zipro1 protein expression increased in CST after denervation.

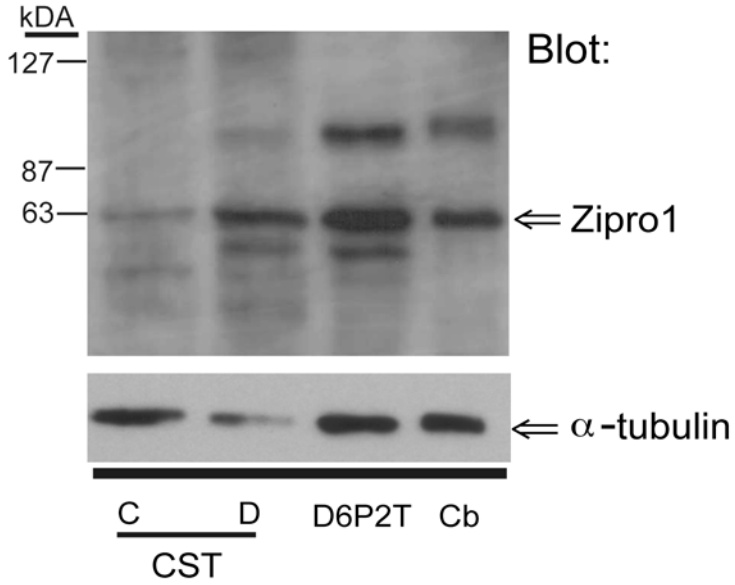

Figure 2.3. Zipro1 protein expression increased in CST after denervation. CSTs were denervated unilaterally in adult rats and removed after 4 days. Seventy five μg of control (C) and denervated (D) homogenized CSTs were run on a SDS-PAGE gel and blotted with Zipro1 antibody. A more intense band at around 63 kDa is seen in D versus C CST. A slightly smaller band, possibly an isoform of Zipro1 (see discussion), is also stronger in D CST. Seventy five μg of a SC line (D6P2T) and Cb extracts were also run. For normalization, the blot was stripped and re-probed with an antibody against α- tubulin. Quantification by densitometry revealed a 2.2 fold increase in Zipro1 expression in D CST. Similar results were observed with 3-day denervated CST (data not shown).

Cellular source of Zipro1 in the CST

Antibody staining of cross sections of the CST revealed two morphologically separate cell populations. Using DAPI to co-stain nuclei, one population of Zipro1+ cells had a small, <10 μm, strongly stained nucleus while the other population had a much larger, faintly stained nucleus around 20 μm in diameter (Fig 2.4). The identity of these cells was ascertained by double-labeling CST tissue with antibodies against SV2 and neurofilament (NF) that recognize neurons, and antibodies against GFAP and S100 that

recognize SCs. SV2 and NF consistently labeled cells with larger nuclei (Fig 2.4A-A''') suggesting that they are neurons, while cells with smaller nuclei were associated with the non-nuclear staining of both GFAP (Fig 2.4B-B''') and S100 (data not shown), suggesting that they are SCs. Macrophage staining was also done using an antibody against CD68. Few macrophages were seen and were located only in the endoneurial sheath surrounding the nerve and they were all Zipro1 negative (data not shown). Thus, both non-myelinating SCs and neurons are Zipro1+ in the CST. To further confirm the labeling of non-myelinating SCs by the Zipro1 antibody, we performed whole-mount immunostaining of soleus muscles from S100-GFP mice. In these mice, SCs express GFP (Zuo et al., 2004). We found that terminal SCs, non-myelinating SCs of the neuromuscular junction, also labeled for Zipro1 (Fig 2.5). Consistent with these data, we also found that D6P2T cells, a prototypical Schwann cell line (Bansal and Pfeiffer, 1987), had high expression levels of the same 63 kDa protein found in cerebellum (Fig 2.3).

Fig 2.4 Neurons and SCs express Zipro1 in the CST.

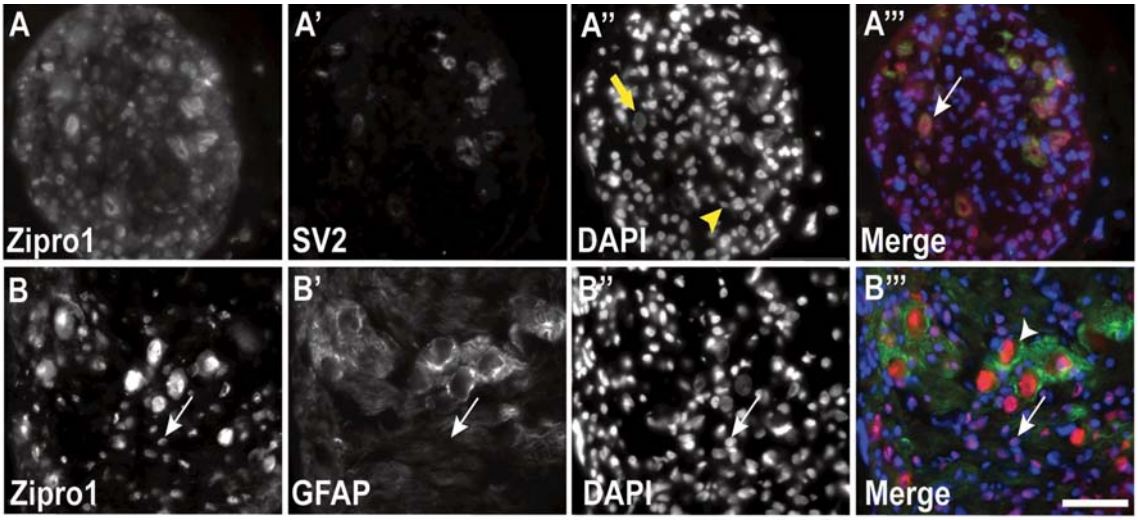

Figure 2.4. Neurons and SCs express Zipro1 in the CST. (A-A'''). Representative Zipro1 staining of large- and small-nucleus cells seen in CST cross-sections (A). A neuronal marker (SV2) only labels the larger cells (A') and this overlaps with Zipro1 staining. The white arrow represents a large cell expressing both Zipro1 and SV2 (A'''). Differing sizes of cell nuclei were visualized with DAPI staining (A''). Large, faintly labeled nuclei correspond with SV2 and Zipro1 (yellow arrow, A''), whereas cells with smaller nuclei (yellow arrowhead, A'') are labeled with Zipro1 only (A). (B-B'''). A glial marker (GFAP), that labels SC cell bodies and processes (B'), surrounds the cell bodies of the larger cells leaving a space between the nucleus and GFAP stain (arrowhead). However, GFAP abuts and surrounds the nuclei of the smaller cells, indicating that the smaller cells are the source of the GFAP (arrow, B'''). Scale bar: 50 μm.

Fig 2.5 Terminal SCs express Zipro1.

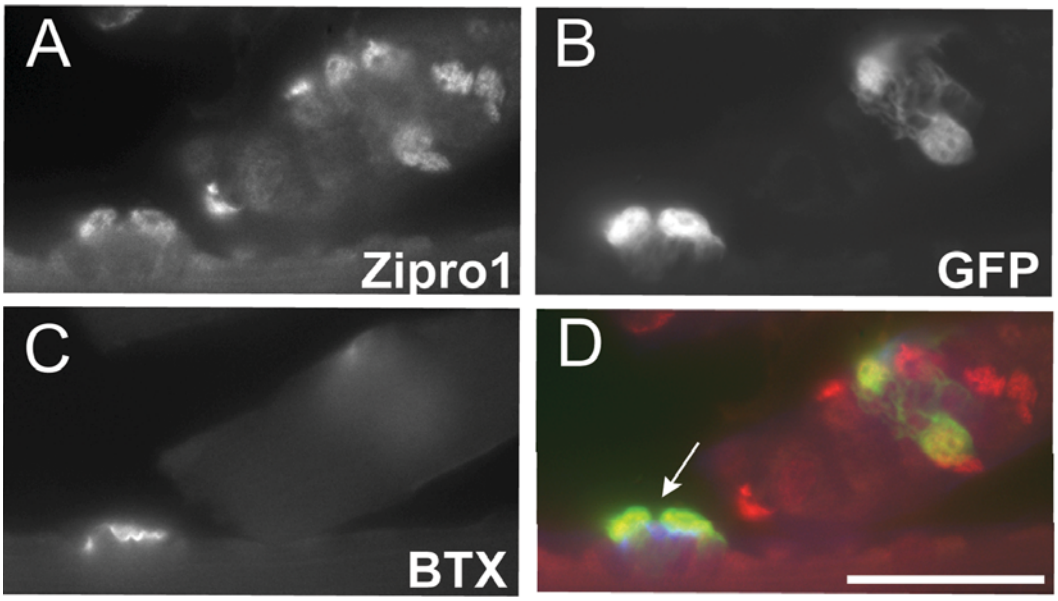

Figure 2.5. Terminal SCs express Zipro1. Whole soleus muscle was removed from a transgenic mouse that expresses GFP (green) in SCs and labeled with Zipro1 (red) and Alexa 647-α -bungarotoxin (BTX) (blue). (A) Zipro1 labels multiple cells at and near a NMJ. Four of the cells also double-label for GFP (D), but only two (arrow, D) are associated with BTX, which labels ACh receptors at the NMJ (D). (B) Four cells are labeled with GFP here, but only the two cells associated with BTX are tSCs (arrow,D). (C) BTX labels one NMJ. (D) The overlay shows the co-expression of GFP and Zipro1 in two tSCs (arrow) on top of BTX staining. Two other cells also co-express GFP and Zipro1. These may be myelinating SCs. Red staining possibly marks myonuclei. Scale bar: 50 μm.

Zipro1 protein is increased in non-myelinating SCs of the denervated CST

Because Zipro1 is expressed in neurons and SCs of the CST, we determined whether the increase seen in Zipro1 was due to changes in expression in neurons, SCs or both. We used a dilution of the Zipro1 antibody (1:5000) that was below saturation for

immunostaining but that still allowed visual detection of the staining in normal CST. At this dilution, we detected an obvious difference between normal and denervated tissue in staining intensity (Fig 2.6A-D). We next used Metamorph imaging software to quantify the average grey value of 335 Zipro1+ SCs and 42 Zipro1+ neurons from both control and denervated CST. A 40% increase in Zipro1 was seen in SCs in the denervated CST, whereas there was no change in Zipro1 expression in neurons (Fig 2.6E). Although smaller, this increase is in line with our previous findings with semi-quantitative PCR and Western blots. The smaller increase may be due to the presence of background fluorescence or to non-linear aspects of the immunostaining. Thus, it appears that non-myelinating SCs account for most, if not all, the change in Zipro1 expression after denervation in the CST.

Fig 2.6 Zipro1 expression levels are higher in SCs of the CST.

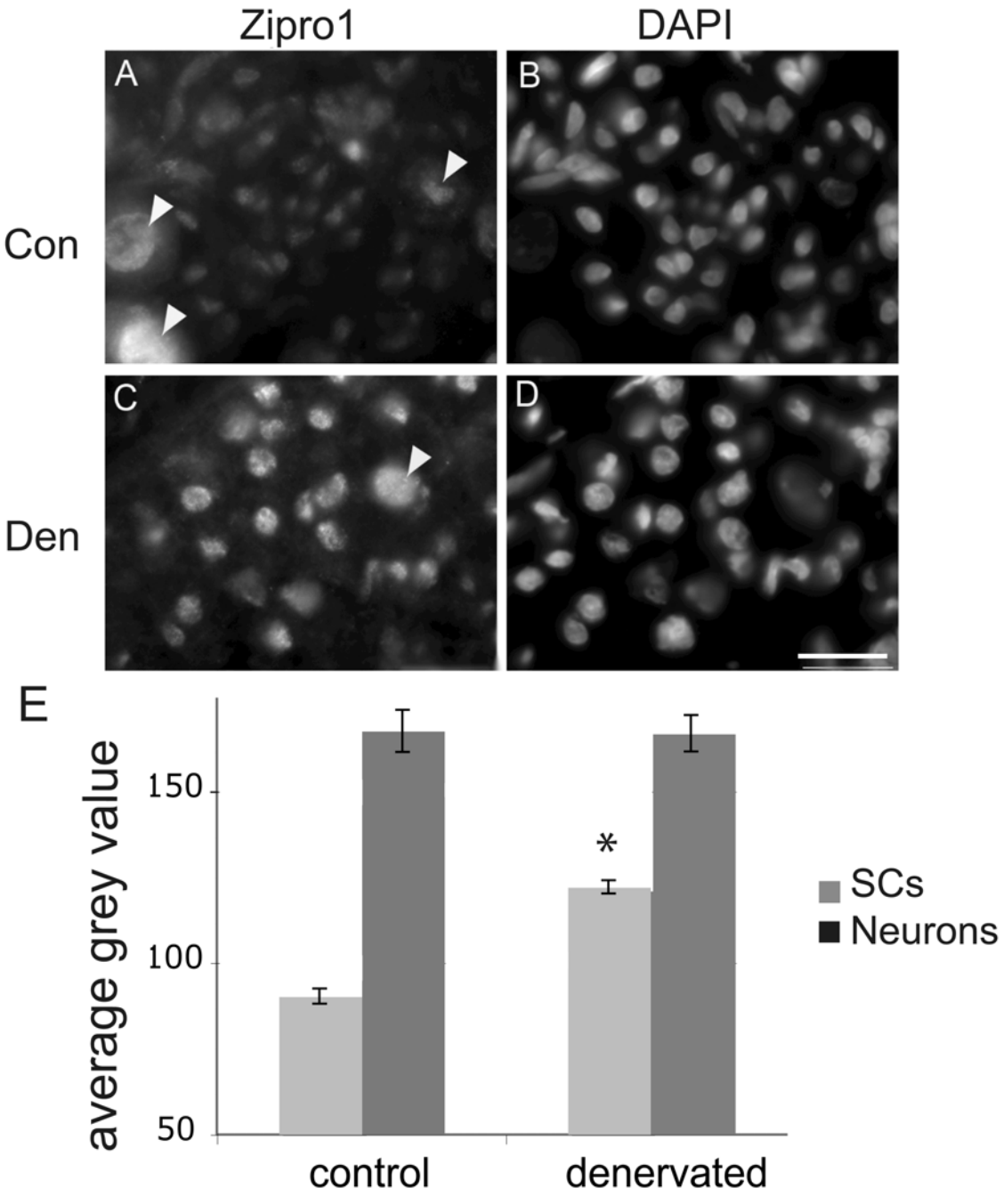

Figure 2.6. Zipro1 expression levels are higher in SCs of the CST. A-D. Cross-sections of control (Con) and denervated (Den) CST were labeled with a non-saturating dilution (1:5000) of Zipro1 antibody. Neurons (arrowheads in A and C) and SCs label for Zipro1 (A,C). Zipro1 staining is brighter in SCs of the Den CST (C). Different size nuclei seen with DAPI staining confirms the identity of SCs versus neurons (B,D). (E) Zipro1 expression in SCs and neurons. Histogram shows average grey values of 335 SCs and 42 neurons from control and denervated CST. Levels were similar for neurons but were significantly different in SCs with a 40% increase in SCs of the denervated CST, suggesting that SCs of Den CST have a significantly higher expression of Zipro1. *, $p < 0.05$, t-test. Scale bar: 50 μm.

Zipro1 protein is increased in tSCs at denervated NMJs

A prime motivation for this study was to identify transcription factor genes that might be involved in tSC activation. Thus, we checked whether Zipro1 was also induced in non-myelinating tSCs following skeletal muscle denervation. We used S100-GFP mice for this experiment as it facilitated the unambiguous identification of tSCs. Using the anti-Zipro1 antibody at 1:5000, we detected a 19% increase in Zipro1 levels in tSCs of denervated synaptic sites (Fig 2.7). Thus, Zipro1 expression also appeared stimulated in tSCs after denervation.

Fig 2.7 Zipro1 expression is higher in denervated tSCs.

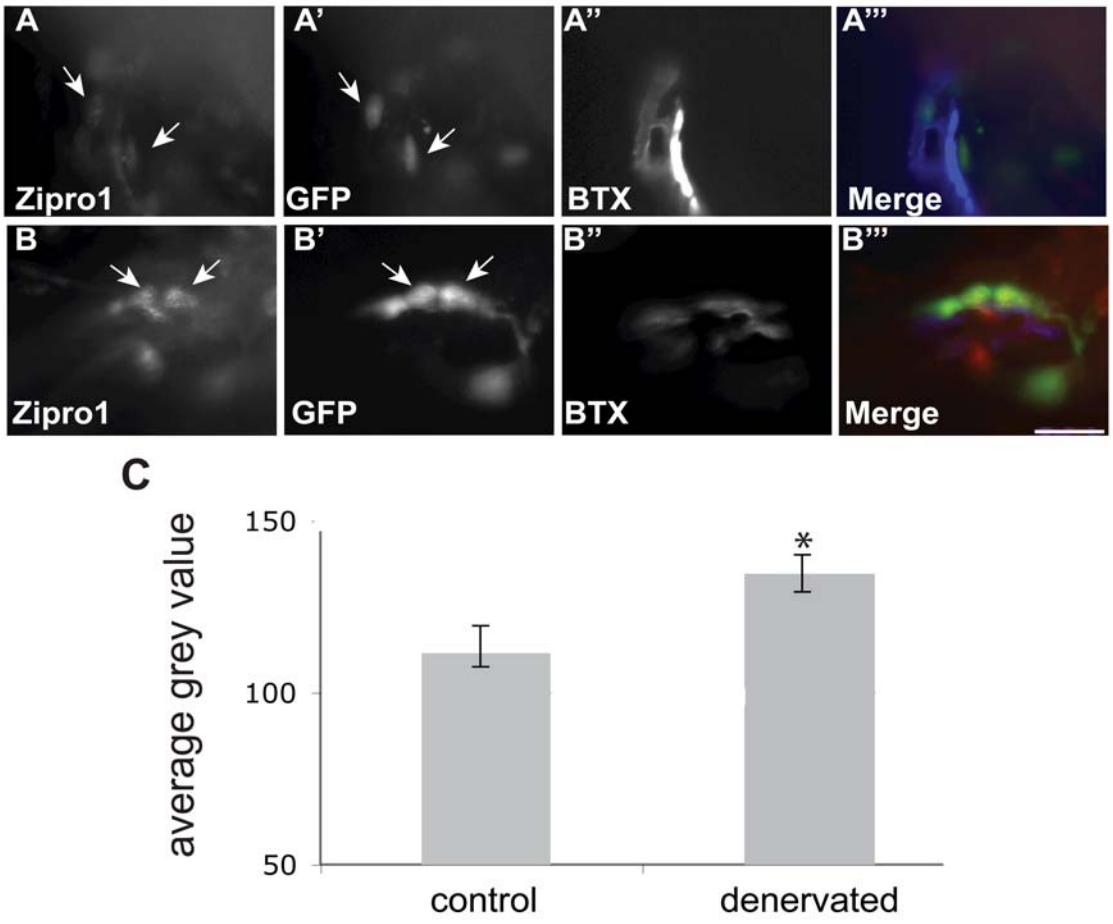

Figure 2.7. Zipro1 expression is higher in denervated tSCs. The sciatic nerve was transected in a S100-GFP mouse and the ipsilateral and contralateral gastrocnemius muscles removed after 3 days. Whole mount tissue was labeled with a non-saturating dilution (1:5000) of Zipro1 antibody. (A-B''') Average grey values were quantified for cells labeled with Zipro1 (arrows, A) and co-expressing GFP (arrows, A') and overlying BTX (A''). Zipro1 labeling is visibly stronger in tSCs of denervated CST. (C) Zipro1 expression in tSCs. Histogram shows average grey values for 38 tSCs in control and denervated muscle. Values were significantly higher by 19% in denervated tSCs suggesting an increase in Zipro1 expression. *, $p < 0.05$, t-test. Scale bar: 25μm.

Discussion

The underlying drive of our research is to discover potential transcription factors that induce tSCs to become reactive. It is in this state that these cells are able to guide axons back to reinnervate an injured NMJ, thus restoring functionality. Using a predominantly unmyelinated nerve, the CST, we looked for potential ZFPs that might have a role in inducing these cells to become reactive. After denervating the CST, we found a two-fold increase of Zipro1 mRNA and protein. We resolved which cells this increase arose from with a previously uncharacterized antibody against Zipro1. We determined that the increase came from the non-myelinating population of SCs in the CST. With the same antibody, we were able to determine that tSCS also express and upregulate Zipro1 after denervation, although the increase was smaller than seen in the SCs of the CST.

The CST is a nerve of the autonomic nervous system that is, for the most part, unmyelinated (98% of unmyelinated nerve fibers (Murata et al., 1982)). While the scarcity of tSCs makes it difficult to isolate their mRNA and protein, the CST provides

adequate levels of mRNA and protein for standard biochemical approaches and it is easily accessible. Here, we assumed that as tSCs and most CST SCs fail to produce myelin and arise from common precursors, they most likely share common transcriptional programs both normally and after denervation. Although our present results seem to bear this assumption out, it is possible that important differences exists as tSCs are associated with motor axons and neuromuscular synapses, while the CST SCs are associated with autonomic axons.

Our ZFP library was built from two independent CST pools, thus, we think it is a good representation of all ZFPs expressed in the normal CST. Nevertheless, it is still possible that there are other C2H2 ZFP genes that escaped detection by our cloning protocol. In particular, we were surprised not to see Egr-1 clones in the CST library. Previously, Topilko et al. (Topilko et al., 1997) found that Egr-1 is expressed by non-myelinating SCs and is upregulated after denervation. As mentioned above, we decided to focus first on Zipro1 because it was the most abundant sequence in our library. However, it is possible that other genes in this library may play more critical roles in non-myelinating SCs. Three of these genes, ZFP111, ZFP180 and U27186, may be good candidates to study next, as they are also expressed in oligodendrocytes (Pott U, 1995; Pott U, 1996).

The cDNA for Zipro1 encodes a zinc-finger transcription factor-like protein. Zipro1's DNA-binding to a bipartite nucleotide sequence has been shown in vitro and in vivo (Yang et al., 1996). Transcription stimulation of a reporter induced by Zipro1 has been demonstrated in cultured cells (Chowdhury et al., 1992). Both Zipro1 mRNA and protein (by Western analysis) increased about 2-fold after denervation. Although this increase might not be that impressive in absolute terms, it is all relative to what this

means for the downstream targets of Zipro1, which at the moment remain unknown. It is possible that a small increase in Zipro1 has a large impact on the expression of downstream target genes. It is tempting to speculate that among these, there might be genes previously reported to be stimulated in tSCs after denervation such as nestin (Kang et al., 2007), GFAP (Georgiou et al., 1994), growth-associated protein-43 (Woolf et al., 1992), and the nerve growth factor low-affinity receptor p75 (Hassan et al., 1994). Very little is known about genes expressed by normal CST SCs, much less about those whose expression changes after nerve injury. An increase in GFAP mRNA was found in the SCG two days after transection of the CST (Boeshore et al., 2004). Although it was not shown that this increase was restricted to glial cells in the SCG, it is likely to be so. This finding suggests that GFAP levels may also increase in CST SCs after nerve injury.

Using immunostaining with a previously uncharacterized commercial antibody, we were able to show that there were two populations of Zipro1+ cells in the CST and that the increase in Zipro1 occurred in cells that co-labeled with SC but not with neuronal markers. Using the same antibody we showed that tSCs also express Zipro1 and that its levels increased there after denervation as well. Neuronal cell bodies that extend into the caudal segments of the rat CST have been previously reported (Bowers and Zigmond, 1981). The fact that CST neurons are Zipro1+ is not surprising as granule cells in the cerebellum and other regions of the brain have been reported to be Zipro1+ by in situ hybridization by others (Yang et al., 1996) and ourselves (Fig 2 and data not shown). Several lines of evidence support the specificity of the immunostaining with the commercial antibody used here. (i) The antibody was raised against a short peptide in the non-zinc-finger domain of Zipro1. (ii) No other significantly similar sequences were found when we BLASTed the epitope sequence (SNLTKHRRTHTGEKPY) in

GeneBank (data not shown). (iii) The staining was nuclear as expected for a transcription factor such as Zipro1. (iv) In the cerebellum, the immunostaining was strongest in the IGL, where we found that the Zipro1 mRNA in situ signal was the strongest as well. (v) In Western blots the strongest band was the one matching Zipro1's expected molecular weight (about 63 kDa). (vi) High levels of Zipro1 expression have been reported in brain and testis by several groups (Chowdhury et al., 1992; Yang et al., 1996). However, while Yang and co-workers failed to detect Zipro1 transcript in other peripheral tissues by Northern analysis on total RNA, Chowdhury et al. detected weak Zipro1 expression in these tissues by Northern analysis of polyA+ enriched RNA. Thus, it is perhaps not surprising that we detected weak Zipro1 levels in peripheral tissues by Western analysis (Fig 2). (vii) The antibody dilution (1/5000) used to estimate the Zipro1 staining differences between control and denervated CST and tSC samples (Figs 6 and 7), was an order of magnitude higher than that used for Western blotting (1/350). This not only allowed us to work outside the saturation range of the antibody but also likely improved the specificity of the staining. Zipro1 is by no means a non-myelinating SCs-specific transcript. In fact, we also detected Zipro1 in myelinating SCs of intramuscular nerves, however, Zipro1 levels decreased after denervation in these cells (data not shown). Thus, we show here that Zipro1 expression is selectively stimulated in non-myelinating SCs after denervation.

To our knowledge, Zipro1 is the first transcription factor reported to be induced in tSCs after denervation. As Zipro1-/- mice are viable and fertile (Yang et al., 1999), it will be interesting to determine whether the absence of this transcription factor alters the response of tSCs to muscle denervation.

Acknowledgements

This work was supported by NIH Grants GM065797 (MR) and NS20480 (WJT), and by start-up funds from TAMHSC (MR). We are grateful to Nigel Atkinson, Ted Mills and Harold Zakon for their encouragement and many useful suggestions. We thank Rick Aldrich for financial support for ELE to finish the experimental phase of this work.

References

Aguayo AJ, Bray GM, Terry LC, Sweezey E. 1976. Three dimensional analysis of unmyelinated fibers in normal and pathologic autonomic nerves. J Neuropathol Exp Neurol 35(2):136-51.

Alonso MB, Zoidl G, Taveggia C, Bosse F, Zoidl C, Rahman M, Parmantier E, Dean CH, Harris BS, Wrabetz L and others. 2004. Identification and characterization of ZFP-57, a novel zinc finger transcription factor in the mammalian peripheral nervous system. J Biol Chem 279(24):25653-64.

Bansal R, Pfeiffer SE. 1987. Regulated galactolipid synthesis and cell surface expression in Schwann cell line D6P2T. J Neurochem 49(6):1902-11.

Bowers CW, Zigmond RE. 1981. Sympathetic neurons in lower cervical ganglia send axons through the superior cervical ganglion. Neuroscience 6(9):1783-91.

Braissant O, Wahli W. 1998. A simplified in situ hybridization protocol using non-radioactively labeled probes to detect abundant and rare mRNAS on tissue sections. Biochemica 1:10-16.

Chowdhury K, Goulding M, Walther C, Imai K, Fickenscher H. 1992. The ubiquitous transactivator Zfp-38 is upregulated during spermatogenesis with differential transcription. Mech Dev 39(3):129-42.

Jessen KR, Mirsky R. 2002. Signals that determine Schwann cell identity. J Anat 200(4):367-76.

Kang H, Tian L, Son YJ, Zuo Y, Procaccino D, Love F, Hayworth C, Trachtenberg J, Mikesh M, Sutton L and others. 2007. Regulation of the intermediate filament protein nestin at rodent neuromuscular junctions by innervation and activity. J Neurosci 27(22):5948-57.

Kang H, Tian L, Thompson W. 2003. Terminal Schwann cells guide the reinnervation of muscle after nerve injury. J Neurocytol 32(5-8):975-85.

Klug A. 2005. Towards therapeutic applications of engineered zinc finger proteins. FEBS

Lett 579(4):892-4.

Murata Y, Shibata H, Chiba T. 1982. A correlative quantitative study comparing the nerve fibers in the cervical sympathetic trunk and the locus of the somata from which they originate in the rat. J Auton Nerv Syst 6(3):323-33.

Pott U, Colello RJ, Schwab ME. 1996. A new Cys2/His2 zinc finger gene, rKr1, expressed in oligodendrocytes and neurons. Brain Res Mol Brain Res 38(1):109-21.

Pott U, Thiesen HJ, Colello RJ, Schwab ME. 1995. A new Cys2/His2 zinc finger gene, rKr2, is expressed in differentiated rat oligodendrocytes and encodes a protein with a functional repressor domain. J Neurochem 65(5):1955-66.

Reddy LV, Koirala S, Sugiura Y, Herrera AA, Ko CP. 2003. Glial cells maintain synaptic structure and function and promote development of the neuromuscular junction in vivo. Neuron 40(3):563-80.

Rimer M, Cohen I, Lomo T, Burden SJ, McMahan UJ. 1998. Neuregulins and erbB receptors at neuromuscular junctions and at agrin- induced postsynaptic-like apparatus in skeletal muscle. Mol Cell Neurosci 12(1-2):1-15.

Rimer M, Prieto AL, Weber JL, Colasante C, Ponomareva O, Fromm L, Schwab MH, Lai C, Burden SJ. 2004. Neuregulin-2 is synthesized by motor neurons and terminal Schwann cells and activates acetylcholine receptor transcription in muscle cells expressing ErbB4. Mol Cell Neurosci 26(2):271-81.

Schaeren-Wiemers N, Gerfin-Moser A. 1993. A single protocol to detect transcripts of various types and expression levels in neural tissue and cultured cells: in situ hybridization using digoxigenin-labelled cRNA probes. Histochemistry 100(6):431-40.

Topilko P, Levi G, Merlo G, Mantero S, Desmarquet C, Mancardi G, Charnay P. 1997. Differential regulation of the zinc finger genes Krox-20 and Krox-24 (Egr-1) suggests antagonistic roles in Schwann cells. J Neurosci Res 50(5):702-12.

Yang XW, Wynder C, Doughty ML, Heintz N. 1999. BAC-mediated gene-dosage analysis reveals a role for Zipro1 (Ru49/Zfp38) in progenitor cell proliferation in cerebellum and skin. Nat Genet 22(4):327-35.

Yang XW, Zhong R, Heintz N. 1996. Granule cell specification in the developing mouse brain as defined by expression of the zinc finger transcription factor RU49. Development 122(2):555-66.

Zuo Y, Lubischer JL, Kang H, Tian L, Mikesh M, Marks A, Scofield VL, Maika S, Newman C, Krieg P and others. 2004. Fluorescent proteins expressed in mouse transgenic lines mark subsets of glia, neurons, macrophages, and dendritic cells for vital examination.J.Neurosci24(49):10999-100

CHAPTER 3: ADDITIONAL FINDINGS ON ZFPS AND NON-MYELINATING SCHWANN CELL ACTIVATION

Chapter 2 contained results and data that were submitted to a peer-reviewed journal. There are additional results that were not included in the manuscript and these appear in this chapter. Some of these results support the main finding in chapter 2, that after denervation there is selective upregulation of Zipro1 in tSCs and non-myelinating SCs of the CST. Other results pertain to different ZFPs, besides Zipro1, that I examined.

Increase in Zipro1 expression in CST is not due to an increase in Schwann cells or neuron number

After showing an increase in Zipro1 levels in denervated CST, I checked whether this increase was due to an overall increase in the number of SCs. To do this, I stained 12 μm sections of control and denervated CST with SV2, to label neurons, and Zipro1, which labels both neurons and SCs. I counted all cells that stained for SV2 and Zipro1 and all cells that stained for Zipro1 only. I found no significant difference in the number of Zipro1-labeled SCs between control and transected CST (Fig 3.1). However, I did find a significantly larger number of Zipro1-labeled neurons in control CST (Fig 3.1, $p<0.05$, two-tailed t-test). An increase of Zipro-labeled neurons should, in theory, increase overall Zipro1 levels in control CST. However, despite this, an increase in Zipro1 levels is found in denervated and not in control CST. Thus, my measurement of transcript levels may underestimate the activation of Zipro1 in the denervated nerves.

Fig 3.1 Schwann cell and neuron counts in control and denervated CST.

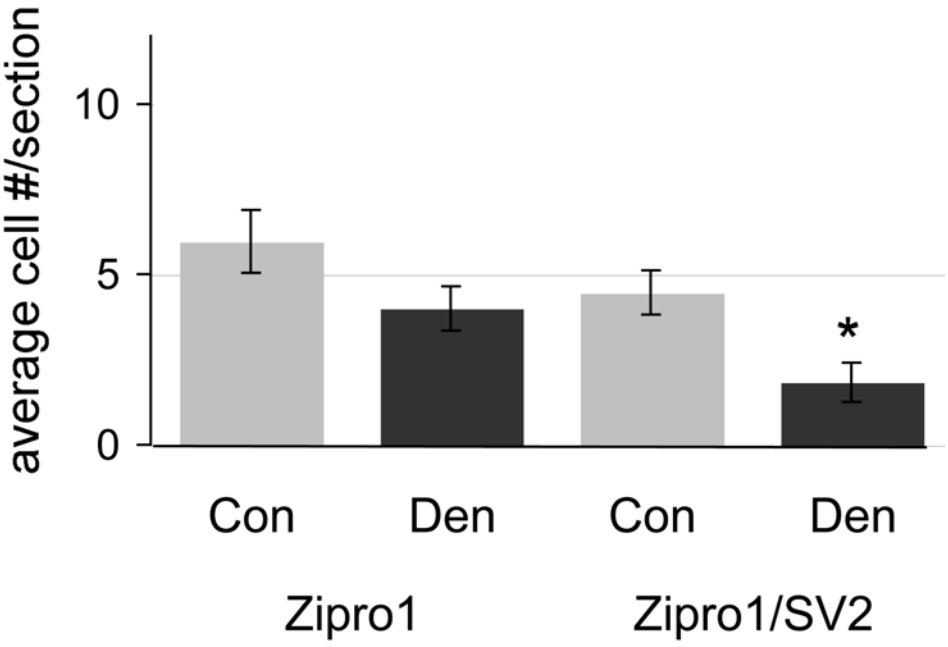

Fig 3.1 Schwann cell and neuron counts in control and denervated CST. 12 μm sections of control and denervated CST were stained with Zipro1, to label SCs, and SV2 antibody, to label neurons. Three circles were placed on top of 25 sections from control and denervated CST. All 3 circles consistently fell within the boundaries of the CST. Cells stained for Zipro1 only and cells stained for Zipro1 and SV2 were counted within these three circles. There is no significant difference between the amount of Zipro1+ SCs in control versus denervated CST. There is a significant difference between the amount of Zipro1+/SV2+ neurons. found in CST. *, $p < 0.05$, t-test.

Zipro1 levels are not increased in myelinating SCs in murine tibialis muscle after denervation

The overall aim of this research was to find transcription factors unique to the reactivation of tSCs. Using whole mount murine tibialis from a transgenic mouse that expresses GFP in SCs, I stained for Zipro1 and quantified fluorescence intensities of

myelinating SCs in both denervated and control muscle. I used a dilution of the Zipro1 antibody (1:5000) that was below saturation for immunostaining but still allowed for visual detection of staining in normal muscle. I then used Metamorph imaging software to quantify the average grey value of 83 Zipro1 positive, myelinating SCs from both control and denervated tibialis. At this dilution, I found a slight decrease in Zipro1 expression in the myelinating SCs of the denervated tibialis. Although slight, this difference was still significant with a $p < 0.05$ (Fig 3.2). Myelinating SCs were distinguished from non-myelinating tSCs by their location. Both myelinating and tSCs express GFP, however, GFP positive cells at a NMJ (this is determined by bungarotoxin staining which labels AChRs at the junction) were considered tSCs. For this experiment, only GFP positive cells not associated with bungarotoxin were evaluated. Thus, it seems that following denervation, Zipro1 levels increase only in non-myelinating SCs, including tSCs.

Fig 3.2 Zipro1 expression in myelinating SCs.

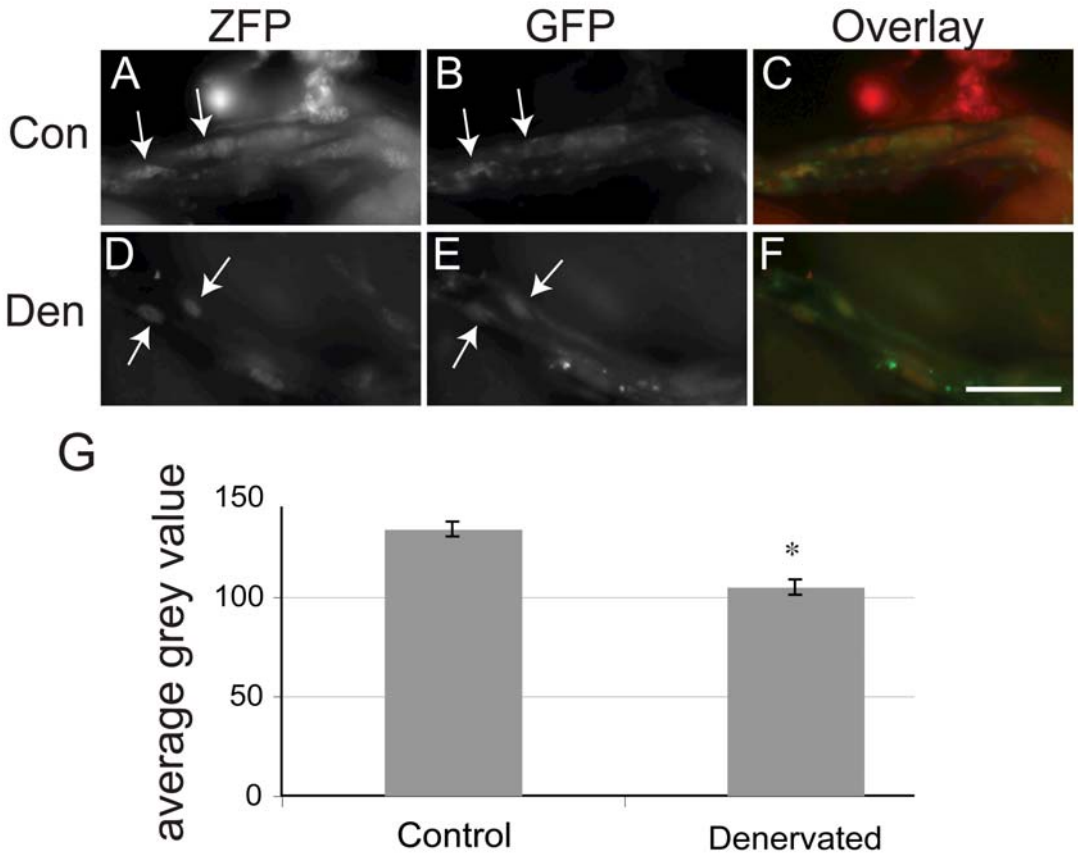

Fig 3.2. Zipro1 expression in myelinating SCs. (A-F). The sciatic nerve was transected in a S100-GFP mouse and the ipsilateral and contralateral gastrocnemius muscles removed after 3 days. Whole mount tissue was labeled with a non-saturating dilution (1:5000) of Zipro1 antibody. (A-F). Average grey values were quantified for cells labeled with Zipro1 (arrows, A & D) and co-expressing GFP (arrows, B & E) in both control (A-C) and denervated (D-F) tibialus. Zipro1 labeling is similar in myelinating SCs of the denervated tibialis and in control tibialus. (G). Histogram shows average grey values for 83 myelinating SCs in both control and denervated muscle. There is a slight, but significant, decrease in Zipro1 expression in myelinating SCs of the denervated samples. Scale bar: 50μm.

Construction of a cDNA library from denervated CST

I had previously constructed a cDNA library from control CST. I also constructed a cDNA library from denervated CST RNA using the same procedure described in chapter 2. Fifty colonies were selected for sequencing. A complete list of both control and denervated genes are listed in table 2. Genes in **bold** appeared in both control and denervated libraries, those in *italics* were found in the denervated library only. Accessions numbers with a strike-through are records that have been recently removed by NCBI as a result of standard genome annotation processing. Another eighteen genes were uncovered in the denervated library, eight of these genes overlapped with the control library. *Zfp629* appeared twelve times and *Zfp160* appeared 8 times suggesting that both of these genes may be upregulated after denervation. Little is known about either of these ZFPs other than they are able to bind DNA and affect transcription (http://www.informatics.jax.org). Structurally, *Zfp160* contains 18 zinc-finger domains and one Kruppel-associated box (KRAB) domain, a transcriptional repressor. KRAB domain. *Zfp629* has 19 zinc-finger domains and is expressed in the mouse retina, and in both central and peripheral nervous systems (Blackshaw et al., 2004).

Table2:Zinc-finger library prepared from control and denervated adult rat CST

Table 2. Zinc-finger library prepared from control and denervated adult rat CST

Insert	Colonies sequenced	Homolog to (Accession #)	Gene name (and other names in literature)	Reported expression in glial cells?	References
1	8	NM_001012021	Zipro1 (Ru49, Zfp38)	No; cerebellum, skin, and testes	1, 20
2	3	NM_001025760	Zfp36 (KOX 18, ZNF 139)	No; encodes for tristetraprolin in fibroblas	2
3	3	NM_011762.3	Zfp 59	No; detected in mature sperm	3
4	3	BC079015	ZNF 61	No; detected in testis cDNA library	4
5	4	NM_133323.	Zfp111	Oligodendrocytes	5
6	1	NM_144757	Zfp180 (rKr1)	Oligodendrocytes (and neurons)	6
7	2	XM_573110.	ZNF 286 (KIAA1874)	?	-
8	3	~~XM_677778~~	ZNF 545 (Zinc finger protein 30 homolog)	?	-
10	1	NM_001014158.	3110052M02Rik protein (similar to KRAZ1)	?	9
11	1	NM_023988.	Znf 354c	No; bone	11
12	1	XM_344876	Zfp74(KRAB8, Zfp66)	No; cardiomyocytes	12
13	1	BC082594	Zfp449	No	14
14	1	~~XM_574417~~	Zfp569	?	-
15	1	AK143471	Zfp30 (KOX28)	Ubiquitous	15
16	2	BC079105	Zfp426	?	16
17	1	U27186	Cys2/His2 zinc finger protein (rKr2)	Oligodendrocytes	17
18	2	NM_001033355	Zfp568	?	18
19	2	NM_027264	Zfp715	?	19
20	1	~~XM_898030~~	RIKEN cDNA 5730601F06	?	-
21	1	~~XM_577790~~	RIKEN cDNA 2610020C11	?	-
22	1	XM_221920	Rattus norvegicus similar to RB-associated KRAB	?	-
23	**6**	**NM_001107428**	**Zfp612**	**No; predominantly kidney**	**7**
24	**4**	**XM_001078438.**	**Znf167**	**?**	**-**
25	**3**	**NM_001106792.**	**ZNF 641 (FLJ31295)**	**No; cancer cell lines**	**8**
26	**2**	**XM_574405.**	**Zfp354A (RIKEN cDNA C030039L03 gene, mous**	**No; predominantly kidney and eye**	**10**
27	**4**	**BC040201**	**Zfp715**	**Ubiquitous**	**13**
28	**6**	**XM_577757.**	**MkIAA1431protein (Zfp28)**	**?**	**-**
29	***5***	**BC079105**	***Zfp426***		
30	**8**	**XM_574381.**	**ZFP235**	**?**	**-**
31	*1*	*XM_001066564*	*LOC683571*	?	-
32	*2*	*NM_001013141*	*Zfp239*	?	-
33	*1*	*NM_018791*	*Zfp108*	?	-
34	*1*	*NM_001107487.*	*Zfp112*	Brain	21
35	*12*	*NM_001107551.*	*Zfp629*	Retina, CNS & PNS	24
36	*1*	*BC035197.*	*Zfp719*	?	-
37	*1*	*NM_001012128.*	*Zfp105*	No; testes	22
38	*1*	*NM_011754.*	*Zfp27*	?	-
39	*1*	XM_001078842.	Zfp14	No; Pancreatic cell line.	23
40	*8*	*BC015291.*	*Zfp160*	?	-
	110				

References

1 Nat Genet. 22(4):327-35 (1999)
2 Proc. Natl. Acad. Sci. U.S.A. 99 (26), 16899-16903 (2002)
3 Cell Growth Differ. 6 (8), 1037-1044 (1995)
4 Proc. Natl. Acad. Sci. U.S.A. 99 (26), 16899-16903 (2002)
5 J. Neurochem. 65 (5), 1955-1966 (1995)
6 Brain Res. Mol. Brain Res. 38 (1), 109-121 (1996)
7 PNAS 98(5):2199-2204 (2000)
8 Nature Genetics 24: 227-34 (2001)
9 Proc. Natl. Acad. Sci. U.S.A. 99 (26), 16899-16903 (2002)
10 Exp. Eye Res. 64 (2), 287-290 (1997)
11 J. Biol. Chem. 276 (21), 18282-18289 (2001)
12 Science 309:1564-1566(2005).
13 Proc. Natl. Acad. Sci. U.S.A. 99 (26), 16899-16903 (2002)
14 Proc. Natl. Acad. Sci. U.S.A. 99 (26), 16899-16903 (2002)
15 New Biol. 2:363-374(1990); Science 309 (5740), 1564-1566 (2005)
16 Proc. Natl. Acad. Sci. U.S.A. 99 (26), 16899-16903 (2002)
17 J. Neurochem. 65 (5), 1955-1966 (1995)
18 Genome Res. 11 (9), 1553-1558 (2001)
19 Gene 213 (1-2), 55-64 (1998)
20 Mech. Dev. 39 (3):129-42. (1992)
21 Science (306):2255-2257 (2004)
22 Mamm. Genome. (9)758-62 (1998)
23 Cancer Lett. 105 (2), 225-231 (1996)
24 PLoS Biol. 2004 Sep;2(9):E247.

Table 2. Library of ZFPs from control and denervated CST. ZFPs found in denervated library only are in italics. ZFPs whose accession number has a strike-through are records that have been recently removed by NCBI as a result of standard genome annotation processing.

Preliminary semi-quantitative PCR shows no mRNA increase for Zfp180, Zfp111, Zfp612, and Zfp36 in denervated CST

As well as looking at *Zipro1* and *Zfp36* (see results from chapter 2), I also looked at three other genes that appeared multiple times in my control CST cDNA library (Table 2.1). These genes included *Zfp180, Zfp111*, and *Zfp612*.

We denervated the CST unilaterally in five adult rats and then after three days removed the nerves from both the denervated and contralateral side. The denervated and control nerves were pooled separately. Total RNA was isolated from these pools and RT-PCR was performed to create cDNA. We designed primers for *Zfp180, Zfp111* and *Zfp612* to look for differential expression in control and denervated CST cDNA. One ug of total RNA from both control and denervated CST was reverse-transcribed to create cDNA. For *Zfp612*, 1/10 of the cDNA reaction was amplified through PCR and the samples ran on a 1% agarose gel. A picture was captured from the gel and visually inspected. There appeared to be no upregulation of *Zfp612* as the band for control and denervated CST were similar in intensity (data not shown). For *Zfp180* and *Zfp11*1, cDNA was amplified in both normal and denervated CST using three separate dilutions (1/5, 1/25, 1/625) in an end-point PCR reaction. There was no difference in band intensity at the lowest dilution in both control and denervated CST for Zfp180 (Fig 3.3) and for Zfp111 (data not shown). A house keeping gene, *β-actin,* was also run at the same time for normalization purposes (Fig 3.3). Because this preliminary end-point PCR results showed no upregulation of these genes in denervated CST, I did not study them further. Nevertheless, these results further support the notion of a selective increase in *Zipro1* expression after transection of the CST.

Fig 3.3 Semi-quantitative PCR shows no upregulation of *Zfp180* mRNA in denervated CST.

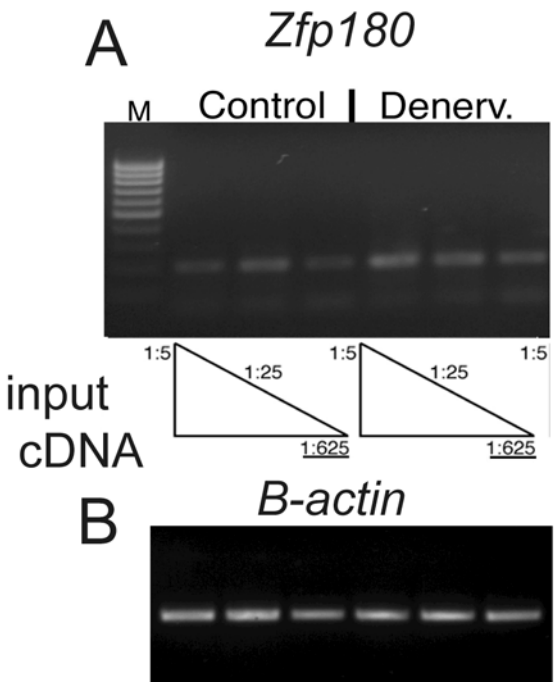

Figure 3.3. Semi-quantitative PCR shows no upregulation of *Zfp180* mRNA in denervated CST. (A) Total RNA was prepared from 3-day denervated CST and contralateral control. One microgram of each sample was reverse transcribed and the resulting cDNA was diluted 1:5, 1:25 and 1:625. Endpoint PCR reactions were carried out with gene-specific primers for *Zfp180* and *β-actin*. Amplified products were run at the same time on 1% agarose gels containing ethidium bromide. For the highest dilution (1:625), where amplification is likely linear, band intensity for *Zfp180* was similar in both samples M: 100-bp size markers. (B*) β-actin* was also amplified in control and denervated samples at the same time as *Zfp180* at the same dilutions, 1:5, 1:25 and 1:625. Theses samples were then run on the same gel with the previous genes as a loading control. All bands for both control and denervated samples have similar intensities indicating that the same amount of cDNA was loaded for both samples

CHAPTER 4: DISCUSSION, CONCLUSIONS AND FUTURE DIRECTIONS

Discussion

The role that reactive tSCs play in the restoration and repair of a damaged neuromuscular junction is a critical one. However, the molecular mechanisms behind the ability of tSCs to become reactive are not known. In fact, little is known about this rare class of non-myelinating SCs. Several zinc-finger transcription factors (ZFPs) have been implicated in various aspects of SC differentiation and development. Therefore, we decided to look within this family of transcription factors for possible candidates that might drive tSCs to become reactive. Because tSCs are few and far between and difficult to isolate, I used another class of non-myelinating SCs as my experimental model. These SCs are derived from the mostly non-myelinated cervical sympathetic trunk (CST). Although these cells may not be identical to tSCs, they should share enough commonality to uncover important molecules that are involved in the reactivation process and eventual reinnervation of the junction.

Construction of cDNA libraries from control and denervated adult rat CST

I was able to construct a library of ZFPs from RNA extracted from both control and denervated CST. Unilateral denervation in rat results in one experimental and one control nerve. I was able to extract an ample amount of RNA from a pool of three-six nerves from both control and denervated CST. Denervated CSTs were removed after three-four days after denervation. As mentioned before, the rodent CST is a nerve of the autonomic system that is, for the most part, unmyelinated (Aguayo, 1973). This means

that a large proportion of RNA from this nerve would be derived from non-myelinating SCs.

We were able to utilize the highly conserved domain of the ZFP -- (Tyr/Phe)-X-Cys-Xm-Cys-X3-Phe-X5-Leu-X2-His-Xo-His-Xn (m is 2 or 4; n is often 5; o is 3 or 4; X is a variable amino acid) -- to pull out only ZFPs from cDNA, prepared from my CST RNA pools, by using degenerate primers designed against this motif. I performed a PCR reaction with the degenerate primers and generated DNA that was subcloned and sequenced. I constructed a library of ZFPs from both control and denervated CST, resulting in a total of 40 unique ZFPs. Ten sequences were unique to the denervated library only. All sequences were from the zinc-finger family emphasizing the stringency of the degenerate primers I used.

Zipro1 is upregulated in denervated CST

I initially focused on ZFPs that stood out amongst my cDNA library. However, many of the ZFPs were and remain uncharacterized. I initially chose to look at ZFPs that were sequenced multiple times. These sequences included *Zipro1, Zfp36, Zfp111, Zfp 180* and *Zfp612*. I also looked at *Zfp629* as it appeared numerous times in the denervated library but not at all in the control library. Using semi-quantitative PCR and after normalizing to a housekeeping gene, ß-actin, I determined that *Zipro1* was increased nearly two-fold in denervated CST. I saw no difference in *Zfp36, Zfp111, Zfp 180* and *Zfp612*. I was unable to make any conclusion for *Zfp629* as each time I performed semi-quantitative PCR I got differing results. I also tried to look for differences in transcript number for *Zfp629* by using real-time PCR. Unfortunately, I could never get a set of primers that showed amplification of *Zfp629* in my samples, even though I saw strong band from the real-time PCR product on an ethidium bromide gel. I also always saw

Zfp629 product with regular PCR.

I wanted to support my semi-quantitative PCR results of *Zipro1* with quantitative PCR, real-time PCR. I initially had a strong result with a four-fold increase in *Zipro1* in denervated CST after normalizing to a house-keeping gene, *18s rRNA*. I saw no increase in *Zfp36,* which is what I expected because of the original semi-quantitative PCR results. This lack of upregulation of *Zfp36* was important to show that there was not a general upregulation of ZFP genes in the denervated CST. After using cDNA from a second set of denervation experiments, I was unable to replicate the original four-fold increase I had seen in the denervated CST sample. The results for the new samples were inconsistent. However, the overall average remained in favor of upregulation in denervated CST, but not in a significant manner. The results for *Zfp36* remained unchanged. It is unclear why my results changed with the second set of cDNA. It is possible that my ability to dissect the CST from the rat had improved over time so that by the time of the second round of experiments, the result was a cleaner prep of CST. However, I performed semi-quantitative PCR with a second and third set of cDNA, resulting in a near two-fold increase of *Zipro1* in denervated CST, similar to results from the first set of cDNA.

I performed Western blots using a commercial Zipro1 antibody purchased from Affinty Bioreagents. Using both control and denervated CST protein from two more separate pools of denervated and control CSTs, I found a two- fold increase in Zipro1 protein after normalizing to α -tubulin. This supports my original findings of a near two-fold increase in *Zipro1* mRNA using semi-quantitative PCR.

Zipro1 expression in rat and mouse tissues

Previous research by Yang et al (96) used non-radioactive in situs to reveal

expression of *Zipro1* in the internal granule layer of the cerebellum and granule cells in other areas of the brain. They also found *Zipro1* expresssion in skin and were able to produce a hair-loss phenotype with a *Zipro1* over-expressing mouse (Yang, Wynder, Doughty, & Heintz, 1999). Yang et al., using Northern blots, failed to show expression of *Zipro1* in other tissues such as liver, kidney and spleen. I performed non-radioactive in situs using a probe I designed against *Zipro1* and found expression of *Zipro1* mRNA in the internal granule layer of the cerebellum, similar to Yang et al. I also found *Zipro1* staining in larger cells, possibly Bergmann glia and/or Purkinje cells, along the periphery of the internal granule layer. I also found staining in other cells outside of the cerebellum. These cells appeared larger than granule cells. I also looked for *Zipro1* expression in SCs in the muscle and CST using in situ hybridization. I did see what looked like *Zipro1* staining in these tissues, but was never able to replicate this (data not shown). This could have been due to the rapid deterioration of mRNA in the tissue coupled with the usage of a non-radioactive in situ protocol as opposed to a more sensitive radioactive in situ protocol. It could have also been due to problems with the adjustment of temperature and incubation times during the hybridization period, although I did try multiple combinations.

I then looked for Zipro1 expression using the commercial Zipro1 antibody. Looking in sagittal sections of the entire brain, cells from the internal granule layer of the cerebellum were stained strongly along with the larger Bergmann and/or Purkinje cells in the periphery of this layer. I also saw staining of a population of cells in the molecular layer of the cerebellum and also in other larger, unidentified cells in other brain areas (data not shown). Concerned about the specificity of the commercial antibody, I performed Western blots on protein from cerebellum, a tissue shown by Yang et al. and

myself to express Zipro1. These Western blots revealed a strong 63 kDa band, corresponding to the size of the Zipro1 protein. I also found Zipro1 protein expression in liver, kidney and spleen, contrary to Yang et al. results. Looking at other tissues, I found expression in muscle and in a Schwann cell line (D6P2T). This expression was confirmed with PCR using cDNA from D6P2T cells, two muscle lines (C2C12 & Sol8), a kidney line (293T), and also cDNA from primary SCs. A notable characteristic of the Zipro1 antibody is that it labels only cell nuclei. This is consistent with the location of a transcription factor, such as Zipro1. This evidence leads me to believe that the commercial antibody is specific for Zipro1. Differing results between our group and Yang's group could be due to a greater sensitivity of our immunohistochemistry and Western results compared to their Northern blots and in situs.

Since I saw upregulation of *Zipro1* in CST after denervation, I needed to show which cells expressed Zipro1 in the CST. Using cross-sections of CST, I performed immunohistochemistry with the Zipro1 antibody. Nuclear staining occurred in two separate cell populations, one population with a nucleus less than <10 μm in diameter, and another population with a much larger, faintly stained nucleus around 20 μm in diameter. I was able to use two antibodies, SV2 and Neurofilament, to ascertain that the cells with the larger, fainter nuclei were neurons. The identity of the smaller cells was harder to ascertain, however their position overlapped with GFAP staining used to label SCs in rat CST (Fig. 2.4) . This staining patterns suggests that these smaller cells are SCs.

The next step was to look for Zipro1 expression in terminal SCs at the neuromuscular junction. To do this, I used both cross-sections and whole-mounts of muscle obtained from the S100-GFP transgenic mouse. Zipro1 expression was seen in most cells expressing GFP, including terminal SCs. Terminal SCs were identified as GFP

expressing cells on top of neuromuscular junctions. Neuromuscular junctions were visualized using α-bungarotoxin, which labels AChRs. Because Zipro1 expression was seen in SCs of the mostly non-myelinated CST, I expected to find Zipro1 expression in tSCs due to their common lineage. Verifying the expression of Zipro1 in both types of SCs strengthens the idea that the SCs from the CST are a good model for studying tSCs.

Upregulation of Zipro1 is specific to Schwann cells of the CST

It has been shown that denervation can cause SCs to proliferate (Carroll et al., 1997). Therefore it is possible that an increase in SC numbers contributed to the increase of *Zipro1* upon denervation. I counted SCs and neurons contained within a specified area across 25 sections of control and denervated CST. There was no difference in the number of SCs between both groups. I did find a small, but significant, decrease in the number of neurons in the denervated CST, this could be due to neuronal death caused by denervation. These findings support that the overall increase in Zipro1 expression is due to SCs, not neurons, of the denervated CST.

Both neurons and SCs in the CST express Zipro1. Are neurons, SCs or both types of cells contributing to the increase in Zipro1 expression in denervated CST? I found a significant increase of 40% in Zipro1 expression only in SCs of the denervated CST. This difference is not as high as the 200% increase seen in the semi-quantitative PCR results or the Western blot results; however, this difference could be explained by the large variance of background staining seen from image to image or because of the non-linear characteristics of immunostaining. I found no difference in Zipro1 expression in neurons. Therefore, SCs are responsible for the increase of Zipro1 expression seen in the denervated CST.

Terminal Schwann cells show an increase in Zipro1 expression in whole-mount soleus muscle

I used the same approach above to examine changes in Zipro1 expression in tSCs. Controls and denervated muscles from a S100-GFP mouse were stained for Zipro1 and for AChRs to mark NMJs. I found a 19% increase in Zipro1 intensity values of tSCs in the denervated muscle. Once again, levels may not have been as high as seen with semi-quantitative PCR or Western blots because of large variances in background staining and non-linear aspects of immunostaining. Interestingly, the increase in Zipro1 expression appeared restricted to tSCs as myelinating SCs in the same muscle failed to show a significant change in Zipro1 staining. Actually, a small decrease was seen in Zipro1 expression in myelinating SCs of the denervated muscle.

Non-myelinating SCs of the CST vs. tSCs

We chose the CST as our model for tSCs as it is mostly unmyelinated. Obtaining RNA and protein from tSCs is difficult due to the sparseness of cells and their location. It is likely that non-myelinating cells of the CST will share some commonality to non-myelinating tSCs as they both descend from a common precursor. However, there is a possibility that using non-myelinating SCs from the CST will not provide us with an accurate description of tSCs. For instance, functions of *Zipro1* in SCs of the denervated CST may not hold true for tSCs. However, because I found a similar increase in Zipro1 expression in both non-myelinating SCs of the CST and in tSCs of the neuromuscular junction, it is possible that Zipro1 may be playing a similar role in both types of cells.

Future directions

My dissertation research resulted in the identification of a transcription factor,

Zipro1, that is increased in SCs of denervated CST and muscle indicating that it may have a role in the events that occur in SCs after injury. The next step would be to test this hypothesis. This could be done by either over-expressing Zipro1 in culture to see if the resulting phenotype of the transfected cells mimics that of a SC after denervation, or to look for specific genetic markers that are known to be upregulated after denervation, such as *nestin* or *GFAP*. I tried this by transfecting cultured 293t cells with a commercial CMV-driven Zipro1 clone, however, for an unknown reason, the vector we purchased did not overexpress Zipro1 (data not shown). Also, even if this had worked, the endogenous levels of Zipro1 in the SC line we used for these experiments (D62PT) turned out to be very high initially (Fig 2.3). Thus, it is possible that a further increase in Zipro1 afforded by the expression vector would not have altered the phenotype of these cells. To do the overexpression experiments one would have to find SCs with low endogenous Zipro1 levels. Another way would be to overexpress Zipro1 in vivo by creating a mouse using the tetracycline-controlled gene expression system that allows spatial and temporal control of gene expression in vitro and in vivo (Gossen and Bujard, 1992).

Another way to confirm whether *Zipro1* is involved in transcriptional regulation in SCs after injury would be to knock-down its expression in SCs. This could be done in culture using RNA interference in a SC line, such as D62PT. This particular SC line has a constitutively active ErbB2 receptor which mimics the effects of denervation (Hayworth et al., 2006). This could also be done in vivo by microinjecting the RNAi, or an RNAi construct, into specific SCs in a denervated muscle. Changes in phenotype could then be monitored. In the D6P2T line, if Zipro1 is involved, then processes should retract and there should be downregulation of gene markers such as Nestin or GFAP. In the in vivo model, downregulating Zipro1 with RNAi should prevent SCs from becoming reactive.

This would also be observed through morphological changes and monitoring gene transcription levels.

Other ZFPs found in both control and denervated libraries still may prove to be fruitful. Especially those ZFPs found only in the denervated library. Two in particular Zfp629 and Zfp160 appeared multiple times, suggesting that they might be upregulated after denervation. This could be done using semi-quantitative PCR, quantitative PCR and Western blots. In situs or immunohistochemistry could be used to determine the location of expression. If either of these genes showed any upregulation, then overexpression or RNAi would be the next step to see if these genes are involved in reactivation process of SCs in denervated tissue.

Conclusions

The goal of my research was to discover potential molecules that induce tSCs to become reactive. It is in this state that these cells are able to guide axons back to reinnervate an injured junction, thus retaining functionality. Using a predominantly unmyelinated nerve, the CST, we looked for potential transcription factors, from the zinc-finger protein family that might have a role in inducing these cells to become reactive. After denervating the CST, we found a two-fold increase in mRNA and protein levels of the transcription factor *Zipro1,* a zinc-finger protein. We resolved in which cells this increase in *Zipro1* was occurring using a previously uncharacterized antibody against Zipro1. We determined that the increase came from the population of SCs in the CST. With the same antibody, we were also able to determine that tSCs also express and upregulate Zipro1 after denervation, although this increase was smaller then that seen in the SCs of the CST. Although the upregulation of Zipro1 after denervation is small, conducting follow up experiments with Zipro1 might begin to unravel the molecular

process behind tSC activation.

CHAPTER 5: GENERAL METHODS

Animal Surgeries

All surgical procedures and animal care followed institutional and NIH guidelines. Adult male and female Sprague-Dawley rats (95-215 g) were anesthetized by intraperitoneal injection of Nembutol® Sodium Solution (50mg/ml) at a dose of 62 mg/ kg. A ventral mid-cervical incision was made and the cervical sympathetic trunk (CST) was transected at a distance of 2–3 mm caudal to the superior cervical ganglion. Following surgery, animals were allowed to recover for 3 or 4 days. Successful surgeries were demonstrated by ipsilateral ptosis. Animals were then sacrificed by CO2 inhalation and both denervated and intact CSTs were harvested and frozen in liquid N2. For muscle: murine leg muscles were denervated by cutting the sciatic nerve under anesthesia. An injection of a 75 mg/ml ketamine, 5 mg/ml xylazine mixture was administered i.p. for every 100 g in weight. Animals were sacrificed 3–4 days after denervation, and muscles were removed and processed as described below.

Reverse transcriptase-polymerase chain reaction (RT-PCR)

RNA isolation was performed using Trizol® Reagent (Cat. No. 15596-026, Invitrogen, CA). I pooled CSTs and homogenized them in a glass homogenizer in 800 µl of Trizol. The homogenized tissue was left for 5 min at room temp before the addition of 160 μl of chloroform. I then shook the sample vigorously for 15 sec and then incubated it for 2-3 min at room temp. The sample was then centrifuged for 15 min at 12K g at 4ºC. I transferred the top phase to a new tube and mixed it with 400 μl of isopropanol and incubated it on ice for 30 min before centrifuging for 10 min at 4ºC. The supernatant was

removed and 800 μl of 75% EtOH was added to the RNA pellet. I briefly vortexed this mixture before centrifugation for 5 min at 7.5Kg at 4ºC. The pellet was then dried for 5-10 min and then resuspended in 50 μl DEPC water. I treated 500 ng of RNA with DNase as follows: add 1 µl 10x reaction buffer (Roche), 1 µl DNase 1, RNase free (Cat. No. 04 716 728 001, Roche), total RNA (500ng) and add DEPC H20 to 10 µl.

This was incubated for 15 min at room temp before the addition of 1 µl of 25 mM EDTA. I then incubated this for 15 min at 65°C (to inactivate). I performed reverse transcriptase PCR on the DNased treated RNA as follows: add 1 µl Oligo DT (Cat. No. 18418-012, Invitrogen), 1 µl pDN6 random primer, and 1 µl 10mM dNTP mix (Cat. No. 18427-013, Invitrogen). Incubate this for 5 min at 65°C. Then, on ice, add to the mixture 4 µl 5x 1st strand buffer (Invitrogen), 2 µl 0.1 M DTT (Invitrogen), and 1 µl RNase inhibitor (Cat. No. 15518-012, Invitrogen). I then mixed this and spun down briefly. The mixture was then put in a 42°C water bath for 1 min before I added 1 µl SuperScript II (Cat. No. 18064-022, Invitrogen, CA). This was incubated for 50 min at 42°C and then inactivated for 15 min at 65°C.

Isolation of Zinc-finger motif enriched library

I used 2 µl of cDNA, prepared from 500 ng of total CST RNA, and amplified it with degenerative primers against the ZFP motif, CysX2 5' -TGCCCNGAGTGYGGNAAR-3' and H/C 5' -NGGCTTCTCNCCNGTATG-3'. Cycling parameters were 15 min at 95°C, 1 initial cycle for 3 min at 94 °C, followed by 40 cycles for 1 min at 94 °C, 1 min at 48 °C and 1 min at 72 °C, and a final extension for 10 min at 72 °C. (Alonso et al., 2004). I ran the samples in 2% agarose gels and cut out amplified bands between 200-600 bps (usually 4-5 bands were seen). I purified these bands with Qiaex kit (Qiagen, San Diego, CA) and directly subcloned the purified DNA into the

pCR2.1-vector (TA cloning kit, Invitrogen, Carlsbad, CA) to generate a zinc finger motif enriched cDNA library. Cloning protocol is as follows: The amount of PCR product used to ligate into 50 ng of pCR®2.1 vector was determined by this formula that was obtained from Invitrogen's TA kit manual:

$$\text{X ng PCR product} = \frac{\text{(Y bp PCR product)(50 ng pCR®2.1 vector)}}{\text{(size in bp of the pCR®2.1 vector: ~3900)}}$$

[Where X ng is the amount of PCR product of Y base pairs to be ligated for a 1:1 (vector:insert) molar ratio.]

I set up each ligation reaction as follows: x μl of pre-determined amount of PCR product, 1 μl 10x Ligation Buffer (provided with kit), 2 μl pCR®2.1vector (25ng/μl), and sterile water to 9 μl, add 1 μl T4 DNA ligase (4.0 Weiss units) (provided with kit). The reaction was then incubated at 14°C overnight. The next day, the ligation reaction was transformed into One Shot® TOP10 Competent Cells (Invitrogen, CA) as per manufacturer's protocol, with a few modifications as described in the following. I centrifuged one vial of TOP 10 cells briefly and put it on ice to thaw. Half of the contents, 25μl, was placed in a separate tube. Each tube was used for a separate transformation. I added 2 μl of ligation mix to each tube of cells and flicked the tubes gently to mix. These tubes were then incubated on ice for 30 min. They were then heat-shocked in a 42° water bath for 30-45 sec and put on ice. 400 μl of LB was added to each tube and was shaken for 1 hr at 37° at 225 rpm. Of the mixture 50 μl, 100 μl and the pellet, after I spun down the remaining liquid for 30 sec at 1000 g, was spread on X-gal treated LB/agar plates that contained 20 μg/ml kanamaycin and 50 μg/ml ampicillin. The plates were incubated overnight at 37ºC. Using a toothpick, I randomly selected individual clones that did not express X-gal and placed the toothpick in 3 mls of LB + 20

μg/ml kanamaycin and 50 μg/ml ampicillin. These tubes were incubated overnight in a shaker at 37ºC. The next day, I purified the DNA from all tubes that showed ample bacterial growth using QIAprep Spin Miniprep kit (Cat. No. 27106, Qiagen), following the manufacturer's protocol. I performed a restriction digest on the cDNA from each miniprep using Ecor1 and incubating overnight at 37ºC. Each restriction digest was set up as follows: 3 μl cDNA, 2 μl EcoR1 buffer (New England Biolabs), 14.5 μl water and 0.5 μl Ecor1 [100,000 units/ml] (New England Biolabs). I ran the restriction digests on a 1% agarose gel with ethidium bromide. Only samples that had two bands corresponding to the vector (3.9kb) and the insert (100-500bp) were sent to the University of Texas at Austin DNA Sequencing Facility for sequencing. I then compared the sequences to other highly similar sequences using NCBI BLAST.

X-Gal treatment of LB/agar plates:

I spread a thin layer of 2% X-GAL (Cat. No. 7240-90-6, Research Products Int. Corp, IL) diluted in DMF (N-N' dimethyl formamide) onto the surface of pre-set LB/agar (plus antibiotics) plates and then placed them in a 37ºC incubator for 3-4 hours or until most of the liquid was absorbed.

Cell culture and transfections:

The SC line D6P2T (Bansal and Pfieffer 1987) and the human embryonic carcinoma 293T cells were grown in DMEM 1x (Cat. No. 10-017-CV, Mediatech, Inc., VA) with 10% Fetal bovine serum (Cat. No. 100-106, BenchMark™) and 50 µg/ml gentamycin. To overexpress Zipro1, I transfected a Zipro1 clone (inserted in an Express-1 plasmid with a CMV promoter, purchased from ATCC) into both D6P2T and 293T cells. I plated around 5 x 10^4/ml to 8 x 10^4/ml cells per 2 ml in a 35 mm culture

dish cells and incubated overnight in a tissue culture incubator. For transfection, I added 3 μl of Fugene 6 (Cat. No. 11 814 443 001, Roche) directly to 97 μl of DMEM with care not to touch the sides of the tubes. The tube was mixed by flicking and incubated for 5 min at room temp. I then added a total of 2 μg of cDNA (experimental: 1 μg Zipro1 clone cDNA, 1 μg pGreen Lantern GFP plasmid (Invitrogen); control: 1 μg pGreen Lantern and 1 μg control plasmid) to this mixture and incubated it for 15-45 min at room temp. The cells that had been incubated overnight were checked to make sure that they were between 50-80% confluent and then fresh media was added. I added the Fugene6/ DNA mixture in a drop-wise manner into the cell media and then gently swirled the plates to mix. The cells were then incubated for 48 hours before I fixed and stained them for Zipro1 according to the immunohistochemistry protocol in the methods section. Cells used to produce efficiency curves for real-time PCR and those used in Western blots were lysed and processed according to protocols in the methods section.

Antibodies and immunohistochemistry

Antibodies used were as follows: polyclonal antibody raised in rabbit against the peptide sequence SNLTKHRRTHTGEKPY of Zipro1 (ZFP38/RU49) (Cat. No. PA1-17222; Affinty BioReagents, Golden, CO) used at 1:250- 1:5000 dilution. A monoclonal antibody to SV2, used at 1:200 (Developmental Studies Hybridoma Bank, University of Iowa), and a monoclonal antibody to neurofilament (NF), used at 1:250 ,(DH3; Developmental Studies Hybridoma Bank, University of Iowa) was used to mark neurons. A rat anti-mouse antibody to CD68 (Cat. No. MCA19578; Serotec), to mark macrophages, was used at 1:50. A polyclonal rabbit antibody to S100β (Cat. No. Z0311, Dako), used at 1:400, anti-glial fibrillary acidic protein (GFAP; Cat. No. G3893; Sigma, St. Louis, MO); used at 1:200. Fluorescein- and Alexa-647- α-bungarotoxin (Cat.

No.B-35450), to mark AChRs, were purchased from Molecular Probes, Eugene, OR; DAPI (Cat. No. D-1306, Molecular Probes, OR) was used to label cell nuclei at 1:1000. Secondary antibodies included goat anti-rabbit rhodamine-conjugated secondary antibody (Cat. No. 111-025-144, Jackson Immunoresearch, West Grove, PA at 1:400 dilution. Fluorescein or Alexa-647 α-bungarotoxin (Cat. No. B-35450), to mark AChRs, was added for the last 20 minutes during the 1 hr incubation period and DAPI was added for the last 2 min.

For frozen sections: Soleus and tibialis muscles and CSTs were pinned on dental wax with steel insect pins then frozen in isopentane cooled in liquid N2. I identified junctional regions by staining a sample set of muscle sections using Karnovsky stain (5mg acetylthiocholine in 6.5 mls Na Hydrogen Maleate, ph 6.0. Then add 0.5 mls 0.1 M Na citrate, 1 ml 30mM CuSO4, 1 ml 5mM K-ferrracyanide in 1 ml H2O). I sectioned 12 μm cross sections with a cryostat and then mounted them on Superfrost Plus Gold microscope slides. I fixed the sections in 1% PFA for 5 min, rinsed in PBS twice for 5 min then rinsed again twice in PBS-T for 5 min before placement in blocker for one hr (blocking solution: 0.5% Triton-100x, 1.5% BSA in PBS). The slides were then incubated with primary antibody at previously mentioned dilutions overnight at 4°C. I rinsed them twice for 10 min in PBS-T before incubating with secondary antibody in blocking solution for 1 hr at room temperature. The junctional regions were visualized with fluorescein- or Alexa-647- α-bungarotoxin at 1:1000 in blocking solution for 45 min to mark AChRs. I added DAPI in the last 5 min of staining at 1:1000 to label cell nuclei. I then rinsed the slides twice for 10 min in PBS-T and twice for 5 min in PBS before coverslipping with Vectashield (Vector Laboratories, Burlingame, CA).

For whole mount: Soleus, gastrocnemius and tibialis muscles were removed and

pinned on a Sylgard dish with steel insect pins. They were then fixed in 4% PFA for 30 min, washed 3 times for 10 min in PBS then once for 10 min in PBS-T. I teased the muscles apart and then blocked them for 30 min in blocking solution (0.5% Triton-100x, 2% BSA in PBS). They were then incubated on a rocker, with primary antibody in blocking solution, overnight at room temp. The next day, I washed them 3 times for 20 min in blocking solution then incubated them in secondary antibody for 1 hr at room temp. I visualized junctional regions with fluorescein- or Alexa-647- α-bungarotoxin used at 1:1000 in blocking solution for 45 min to mark AChRs. I added DAPI in the last 5 min of staining at 1:1000 to label cell nuclei. The muscles were then washed 3 times 20 min in blocking solution, overnight at 4°C in PBS-T and then stored in PBS.

For cell culture: 293T and D6P2T cells were cultured as described in the cell culture section of this section. I removed the media from the cell plates before fixing in 4% PFA for 15 min. I rinsed the cells twice for 15 min in PBS and then twice for 5 min in PBS-T before blocking for 1 hr in blocking solution (3% BSA in TBS-T (0.5%)). I added the Zipro1 antibody in blocking solution, at 1:750 and incubated over night at 4°C with agitation. The next day, I rinsed the cells in PBS-T 3 times for 10 min. The cells were then incubated for 1 hr at room temp in Goat anti-rabbit rhodamine-conjugated secondary antibody at 1:400 in blocking solution. The cells were then washed 2 times in PBS-T for 10 min and 2 times for 5 min in PBS before mounting in Vectashield (Vector Laboratories, Burlingame, CA) and coverslipping.

In situ hybridization

I prepared riboprobes from primers consisting of a clamp sequence, a core promoter and the gene specific sequence. For Zipro1 antisense probe: the clamp sequence was 5'-CAGAGATGCA-3', a T3 core promoter 5'

ATTAACCCTCACTAAAGGGAGA-3' and sequence specific sequence of 5'-CCTTCGCCCATTAAAGTTGA-3' . For Zipro1 sense strand, clamp region was 5' CCAAGCCTTC-3', T7 promoter 5' TAATACGACTCACTATAGGGAGA-3' and gene specific sequence 5'-TTTTGAGTCCACCTGCATGA-3'. For Zfp629 sense strand: the clamp sequence was 5' CAGAGATGCA-3', a T3 core promoter 5' ATTAACCCTCACTAAAGGGAGA-3' and sequence specific sequence of 5'-TGGGAGATCCAGCTCAGAGT-3'. For Zfp629 sense strand, clamp region was 5' CCAAGCCTTC-3', T7 promoter 5' TAATACGACTCACTATAGGGAGA-3' and gene specific sequence 5'-CTGTTCCAGGTGGTGAAGGT-3'. Sequencing parameters were (95°C for 15 min, 3 times at 94°C, 52°C for 2 min, and 72°C for 1.5min, 36 times at 94°C for 1 min, 62°C for 1 min and 72°C for 1.5 min followed by a final extension of 72°C for 5 min). The amplified product was run on a 1% agarose gel. I excised a band from the gel at the correct size and purified it using a minElute PCR purification Kit (Cat. No. 28004, Qiagen) according to manufacturers protocol. I labeled 1 µg of DNA with 2µl DIG labeling Mix (Roche), 2µl 10X transcription buffer, 1µl (20U) RNAse inhibitor and 1µl RNA-polymerase T3 or T7 to a total volume of 20 µl with H2O-DEPC. This was incubated for 1-2h at 37°C. 1µl DNAse (RNAse free) was added for 15 min at 37°C to digest DNA template. I hydrolyzed the probe by adding 56.2 µl of solution A (50 µl 0.1M DTT, 40 µl 1M NaCo3, 60 µl 1M Na2CO3, 350 µl DEPC-H2O) and incubating at 60°C for 45 min. The reaction was stopped by adding solution B (50 µl 0.1M DTT, 100 µl 1M Na- acetate, 5 µl Acetic Acid, 345 µl DEPC-H2O). The probe was precipitated for 45 min at -80°C with the addition of 13.2 ul of 4M LiCl (made in DEPC), 331 ul of 100% EtOH. This was then spun at 4°C for 20 min at 13k g, washed in 70% EtOH (made in DEPC-H2O), spun again at 4°C for 10 min. I then dried and resuspended the pellet in 50 ul of

DEPC-H2O + 50 ul formamide.

Tissue preparation: Soleus and tibialis muscles and CSTs were pinned on dental wax with steel insect pins and a thin layer of Tissue-Tek® Cat. No. 4583, CA) was put on top before freezing in isopentane cooled in liquid N_2. I sectioned 12 μm cross sections with a cryostat and mounted them on Superfrost Plus Gold microscope slides (Erie Scientific Corp., NH). I identified junctional regions in muscle sections with a Karnovsky stain to visualize AChesterase. I drew a ring around sections from the junctional region with a PAP-pen to retain solutions.I then fixed these sections in 4% PFA for 20 min at room temp, rinsed 2 x 15min in 0.1% active DEPC in 1xPBS and 15min in 5xSSC at room temp. before pre-hybridizing for 2h at 58°C. (prehyb solution: 50% formamide, 5xSSC, 40ug/ml salmon sperm DNA). I added 500 -1000 ng of probe from sense and antisense sequences to the prehyb solution and then added the solution to the sections. The slides were sealed in a airtight, humid container and incubated for 48 hrs at 58°C. After 48 hrs, the slides were washed in mailers as follows: 30 min in 2xSSC at room temp, 1 hr in 2xSSC at 65°C. The slides were then equilibrated for 5 min in Buffer 1 (Buffer 1: pH 7.5 Tris 100mM/NaCl 150mM) before incubation with Anti-Digoxigenin-AP (Cat. No.. 11 093 274 910, Roche) at 1:5000 in Buffer 2 (Buffer 2: Buffer1 + 0.5% non-fat dry milk) for 2 hrs at room temp. The antibody should be spun for 2 min at 16K g before adding to buffer. I then washed the slides in Buffer 1 2 x for 15 min, then for 5 min in Buffer 3 (Buffer 3: pH 9.5 Tris 100mM/NaCl 100mM/MgCl2 50mM -this buffer needs to be made fresh each time, since MgCl2 will precipitate). I then set the color reaction overnight (For 15ml Buffer 3; add 67.5ul NBT (Cat. No... 11 681 451 001; Roche) and 52.5 mls BCIP (Cat. No... 11 681 451 001; Roche), and wrapped the mailers in foil to keep them in the dark without agitation. The next day, I stopped the reaction for

15min in TE (pH 8.0). The non-specific binding was removed for 15-60 min in 95% EtOH, depending on the strength of the staining. The slides were then placed in fresh 95%, 100% and then Histo-Clear (for 1 min in each solution) before I mounted them in Eukitt™ Mounting Media (Electron Microscopy Sciences, PA).

Semi-quantitative PCR

Semi-quantitative PCR was performed by collecting aliquots from PCR reactions at different cycles during amplification or with end-point PCR with differing diltuions (1:5, 1:25 & 1:625). Each 25 µl PCR reaction was comprised of 12.5 µl HotStarTaq DNA Polymerase (Ca. No. 203203, Qiagen), 0.5 µl of each forward and reverse primer, and 9.5 µl H20. Sequencing parameters were 95°C for 15 min, 39 times at 94°C for 1 min, 50°C for 30 sec and 72°C for 30 sec, followed by a final extension at 72°C for 10 min. I ran the collected samples on a 1% agarose gel containing ethidium bromide, along with exACTgene 100bp (Cat. No.. BP 257100) and 1 Kb (Cat. No.. BP2578100) DNA ladders (Fisher BioReagents) to determine band size. I captured an image of the gel and the n quantifed the average grey values of the bands using Metamorph 5.0 (Universal Imaging). I graphed the results with the log of average grey values vs. linear cycle numbers. Differences in mRNA values were obtained using linear regression from equations obtained from lines fit to the data points.

Primer sequences were:

Zipro1: Forward 5'- AGT CCC AGG TTT GGA GTG TG-3'; Reverse 5'- GAA GGT CCC AAC TGT TCC AA-3'

Zfp36: Forward 5'-CCC TGT TGG ACT CCA CCT AA-3'; Reverse 5'-GCC TCT TCT CCA CTG TCA GG-3'

Zfp111: Forward 5'-GCA AGG GTT TCA GTC AGA GC-3'; Reverse 5'-CTC TGG TGG GTG TGA AGG TT-3'

Zfp612: Forward 5'-CTG TCC CCT GAA CAG AGA GC-3'; Reverse 5'-AAG TGT GGC ATG GGA CTA GG-3'

Zfp180: Forward 5'-AAA GCC GTA CAA ATG CAA CC-3'; Reverse 5'-GAA CGA CTT CCC ACA CTG GT-3'

Zfp105: Forward 5'- ACC CCT TGG GAG CTA CTC AT-3'; Reverse 5'-CCA GAC AAT GGG CAG TCT TT-3'

Zfp112: Forward 5'-TCT CAG GAC TTC CCA GCA GT-3'; Reverse 5'-GAA CTT GAA GAG CCC GTA TG-3'

Zfp239: Forward 5'- CAT GAA CGT CCG AAA TGT TG-3'; Reverse 5'- TCC ATA GGG CAG AAC TGG AC-3'

Zfp629: Forward 5'- GGA AAG GGC TTC AAT GAT GA-3'; Reverse 5'- CCT TTC GTG AGT GTG GGT TT-3'

β-Actin: F 5'-GCT ACA GCT TCA CCA CCA CA-3'; R 5'-AAG GAA GGC TGG AAA AGA GC-3'

Real-time RT PCR

I only used primers that achieved efficiency values of around 90% and these efficiency curves were created using cDNA dilutions of 50 ng/µl, 1 ng/µl, 0.1 ng/µl, 0.01 ng/µl. Each 25 µl reaction was comprised of 2 µl cDNA, 2x QuantiTect SYBR Green PCR Master Mix (Qiagen), 10x QuantiTect Primer Assay (Qiagen), H20 to 25 µl. Exception: Zipro1 Primer Assay was used at 5x. For Zfp36, each 25µl reaction was

comprised of 2 µl cDNA, 2x QuantiTect SYBR Green PCR Master Mix (Qiagen), 0.75 µl of both forward and reverse primers [20 µM] and 9 µl H20. Primers for Zfp36 were: Forward 5'-CTC ACG GAA CAG TGC AGA AA-3' ; Reverse 5'- GCT TCC CTT GAC TCA GCA GT-3'. QuantiTect Primer Assay (Qiagen) catalog information for Zipro1, GAPDH, 18s ribosomal and Zfp629 are: Zipro1 (Rn_Zipro1_1_SG QuantiTect Primer Assay (200) QT01626009, Qiagen), GAPDH, (Rn_2_SG QuantiTect Primer Assay (200) QT00423122, Qiagen), 18s ribosomal (Rn_Rnr1_1_SG QuantiTect Primer Assay (200) QT00199374, Qiagen), Zfp629 (Rn_LOC308998_1_SG QuantiTect Primer Assay (200) QT00397439, Qiagen). I tried two separate Primer Assay sets of Zfp629 from Qiagen and designed my own set (Forward 5'- CCT CAG CAG GAA AGT TCT GG-3'; Reverse 5'-CTG TTC CAG GTG GTG AAG GT-3'). None of these achieved a high enough efficiency so I did not use them. Each reaction was run on a Stratagene Mx™ QPCR machine. Parameters were as follows: 95°C for 15 min, 35-40 cyles at 94°C for 15 sec, 50°C for 30 sec and 72°C for 30 sec.

Western Blotting

Cerebellum, kidney, liver, skeletal muscle, and both transected and control CSTs, were removed from rats and snap frozen in liquid N2. I homogenized the cerebellum, kidney and liver with a polytron in an ice-cold RIPA buffer with 10% v/v Protease Inhibitor cocktail (Cat. No.. P8340, Sigma, St. Louis, MO) 3 times for 10 sec each. CSTs were homogenized by sonication in the same buffer at medium speed, 3 times for 10 sec each. The extracts were then passed through a 21-gauge needle several times to reduce viscosity and stored at -80°C until use. D6P2T and 293T cells were cultured as previously described in this methods section, rinsed in cold PBS, and scraped from the dish in RIPA buffer with 10% v/v Protease Inhibitor cocktail (Cat. No.. P8340, Sigma, St.

Louis, MO); the cells were broken up by passage of the suspension through a 21-gauge needle several times. I spun the samples down for 10 min at 1000g at 4°C. The supernatants were concentrated using a Centricon YM-30, 30,000 MW cut-off (Millipore Corp., Bedford, MA), following the manufacturer's instructions. I estimated protein concentration using the Bradford-based, Biorad Protein Assay (Biorad, Hercules, CA). The indicated amount of extracts were mixed with 2x Laemmli sample buffer (Cat. No.. S3401-IVL, Sigma, St. Louis, MO), heated for 5 min at 95°C, and fractionated in 7.5% acrylamide denaturing gels along with a Kaleidoscope Protein Standard (Cat. No.. 310001997, Bio-Rad) to mark molecular weights. The running buffer for the gel was [(for 10x solution: For 1 L add 30.3 g Trizma base (0.25 M), 144 g Glycine (1.92 M) and 10 g SDS (1%)]. I transferred the gel to a prepared PVDF membranes for 1 hr at 23 mV. Preparation of PVDF membrane was as follows: 15 sec in methanol, 2 min in H20, 2 min blotting buffer [10x Blotting buffer: 1 L 30.3 g Trizma base (0.25 M) and 144 g Glycine (1.92 M)]. The Western blots were blocked for 1 hr in blocking solution (5% non-fat milk in TBS-T) and probed with Zipro1 antibody, used at 1:350, in blocking overnight at 4°C with agitation (note: to save antibody, the blot can be rolled and placed in a 50 ml conical tube and rotated over night at 4°C. This way needs as little as 3.5 mls total). The next day, I washed the blot 3 times for 15 min before adding Horse Radish Peroxidase-conjugated anti-rabbit secondary antibody (Jackson Immunoresearch, West Grove, PA), at 1:3000 dilution, in blocking solution for 1 hr at room temp. The blot was then washed 3 times 15 min in TBS-T. Antibody-binding was detected by chemiluminescence according to the manufacturer's instructions (cat# NEL103, Perkin Elmer, MA) (I place the blot on a small piece of saran wrap, add 400 µl of each solution, pick up saran wrap and mix by slight agitation for 1 min). The blots were then placed in a cassette with a

BioMax Light Film (Cat. No. 1788207, Kodak) and processed. For normalization, I stripped the membranes for 30 min at 50°C in prewarmed stripping solution (For 500ml of stripping buffer: 3.5ml of 14.3M Beta Mecap; 50ml of 20% SDS; 31.25 1 M Tris-HCL ph 6.8 and 415.25ml of water). I then washed the blot 3 times 5 min in TBS-T before blocking. I then prepared the blot in the same way as described above but with a monoclonal antibody against α-tubulin (T-9026; Sigma, St. Louis, MO) at 1:4000, and a Horse Radish Peroxidase- conjugated anti-mouse secondary at 1:4000(Jackson Immunoresearch, West Grove, PA). For quantification, the film was scanned and images were saved as TIFF files. Optical density measurements were taken from scans of films using MetaMorph 5.0 software (Universal Imaging). The value for denervated CST was divided by the value for the control CST for both Zipro1 and α-tubulin. For normalization, the ratio obtained for Zipro1 was then divided by the ratio for α -tubulin.

REFERENCES

Aguayo, AJ, Epps, J, Charron, L, Bray, GM (1976) Multipotentiality of Schwann cells in cross-anastomosed and grafted myelinated and unmyelinated nerves: quantitative microscopy and radioautography. Brain Res, 104:1–20.

Aguayo, AJ,Bray, GM; Terry, LC; Sweezy, E (1973) Three dimensional analysis of unmyelinated fibers in normal and pathologic autonomic nerves.

Alonso, MB, Zoidl, G, Taveggia, C, Bosse, F, Zoidl, C, Rahman, M, Parmantier, E, Dean, CH, Harris, BS, Wrabetz, L, Muller, HW, Jessen, KR, Mirsky, R (2004) Identification and characterization of ZFP-57, a novel zinc finger transcription factor in the mammalian peripheral nervous system. J Biol Chem, 279:25653–25664.

Araque, A, Parpura, V, Sanzgiri, RP, Haydon, PG (1999) Tripartite synapses: glia, the unacknowledged partner. Trends Neurosci, 22:208–215.

Astrow, SH, Tyner, TR, Nguyen, MT, Ko, CP (1997) A Schwann cell matrix component of neuromuscular junctions and peripheral nerves. J Neurocytol, 26:63–75.

Auld, DS, Robitaille, R (2003) Perisynaptic Schwann cells at the neuromuscular junction: nerve- and activity-dependent contributions to synaptic efficacy, plasticity, and reinnervation. Neuroscientist, 9:144–157.

Bansal, R, Pfeiffer, SE (1987) Regulated galactolipid synthesis and cell surface expression in Schwann cell line D6P2T. J Neurochem, 49:1902–1911.

Bixby, JL, Lilien, J, Reichardt, LF (1988) Identification of the major proteins that promote neuronal process outgrowth on Schwann cells in vitro. J Cell Biol, 107:353–361.

Blackshaw, S, Harpavat, S, Trimarchi, J, Cai, L, Huang, H, Kuo, WP, Weber, G, Lee, K, Fraioli, RE, Cho, SH, Yung, R, Asch, E, Ohno-Machado, L, Wong, WH, Cepko, CL (2004) Genomic analysis of mouse retinal development. PLoS Biol, 2:E247.

Boeshore, KL, Schreiber, RC, Vaccariello, SA, Sachs, HH, Salazar, R, Lee, J, Ratan, RR, Leahy, P, Zigmond, RE (2004) Novel changes in gene expression following axotomy of a sympathetic ganglion: a microarray analysis. J Neurobiol, 59:216–235.

Bowers, CW, Zigmond, RE (1981) Sympathetic neurons in lower cervical ganglia send axons through the superior cervical ganglion. Neuroscience, 6:1783–1791.

Carroll, SL, Miller, ML, Frohnert, PW, Kim, SS, Corbett, JA (1997) Expression of neuregulins and their putative receptors, ErbB2 and ErbB3, is induced during Wallerian degeneration. J Neurosci, 17:1642–1659.

Chowdhury, K, Goulding, M, Walther, C, Imai, K, Fickenscher, H (1992) The ubiquitous transactivator Zfp-38 is upregulated during spermatogenesis with differential transcription. Mech Dev, 39:129–142.

Fawcett, JW, Keynes, RJ (1990) Peripheral nerve regeneration. Annu Rev Neurosci,

13:43–60.

Georgiou, J, Robitaille, R, Trimble, WS, Charlton, MP (1994) Synaptic regulation of glial protein expression in vivo. Neuron, 12:443–455.

Gossen, M, Bujard, H (1992) Tight control of gene expression in mammalian cells by tetracycline-responsive promoters. Proc Natl Acad Sci U S A, 89:5547–5551.

Hassan, SM, Jennekens, FG, Veldman, H, Oestreicher, BA (1994) GAP-43 and p75NGFR immunoreactivity in presynaptic cells following neuromuscular blockade by botulinum toxin in rat. J Neurocytol, 23:354–363.

Hayworth, CR, Moody, SE, Chodosh, LA, Krieg, P, Rimer, M, Thompson, WJ (2006) Induction of neuregulin signaling in mouse schwann cells in vivo mimics responses to denervation. J Neurosci, 26:6873–6884.

Jahromi, BS, Robitaille, R, Charlton, MP (1992) Transmitter release increases intracellular calcium in perisynaptic Schwann cells in situ. Neuron, 8:1069–1077.

Jander, S, Bussini, S, Neuen-Jacob, E, Bosse, F, Menge, T, Muller, HW, Stoll, G (2002) Osteopontin: a novel axon-regulated Schwann cell gene. J Neurosci Res, 67:156–166.

Jessen, KR, Mirsky, R (2002) Signals that determine Schwann cell identity. J Anat, 200:367–376.

Kang, H, Tian, L, Son, YJ, Zuo, Y, Procaccino, D, Love, F, Hayworth, C, Trachtenberg, J, Mikesh, M, Sutton, L, Ponomareva, O, Mignone, J, Enikolopov, G, Rimer, M, Thompson, W (2007) Regulation of the intermediate filament protein nestin at rodent neuromuscular junctions by innervation and activity. J Neurosci, 27:5948–5957.

Kang, H, Tian, L, Thompson, W (2003) Terminal Schwann cells guide the reinnervation of muscle after nerve injury. J Neurocytol, 32:975–985.

Klug, A (2005) Towards therapeutic applications of engineered zinc finger proteins. FEBS Lett, 579:892–894.

Ko, CP, Chen, L (1996) Synaptic remodeling revealed by repeated in vivo observations and electron microscopy of identified frog neuromuscular junctions. J Neurosci, 16:1780–1790.

Levi, AD, Bunge, RP, Lofgren, JA, Meima, L, Hefti, F, Nikolics, K, Sliwkowski, MX (1995) The influence of heregulins on human Schwann cell proliferation. J Neurosci, 15:1329–1340.

Lin, W, Sanchez, HB, Deerinck, T, Morris, JK, Ellisman, M, Lee, KF (2000) Aberrant development of motor axons and neuromuscular synapses in erbB2-deficient mice. Proc Natl Acad Sci U S A, 97:1299–1304.

Murata, Y, Shibata, H, Chiba, T (1982) A correlative quantitative study comparing the nerve fibers in the cervical sympathetic trunk and the locus of the somata from which they originate in the rat. J Auton Nerv Syst, 6:323–333.

Pott U, THJ, Colello RJ, Schwab ME. (1996) A new Cys2/His2 zinc finger gene, rKr1, expressed in oligodendrocytes and neurons. Molecular Brain Research, Volume 38, Issue

1:109–121.

Pott U, THJ, Colello RJ, Schwab ME. (1995) A New Cys2/His2 Zinc Finger Gene, rKr2, Is Expressed in Differentiated Rat Oligodendrocytes and Encodes a Protein with a Functional Repressor Domain. J Neurochem., 65:1955–1966.

Rando, TA, Bowers, CW, Zigmond, RE (1981) Localization of neurons in the rat spinal cord which project to the superior cervical ganglion. J Comp Neurol, 196:73–83.

Reddy, LV, Koirala, S, Sugiura, Y, Herrera, AA, Ko, CP (2003) Glial cells maintain synaptic structure and function and promote development of the neuromuscular junction in vivo. Neuron, 40:563–580.

Rimer, M, Prieto, AL, Weber, JL, Colasante, C, Ponomareva, O, Fromm, L, Schwab, MH, Lai, C, Burden, SJ (2004) Neuregulin-2 is synthesized by motor neurons and terminal Schwann cells and activates acetylcholine receptor transcription in muscle cells expressing ErbB4. Mol Cell Neurosci, 26:271–281.

Robitaille, R (1998) Modulation of synaptic efficacy and synaptic depression by glial cells at the frog neuromuscular junction. Neuron, 21:847–855.

Robitaille, R, Jahromi, BS, Charlton, MP (1997) Muscarinic Ca2+ responses resistant to muscarinic antagonists at perisynaptic Schwann cells of the frog neuromuscular junction. J Physiol, 504:337–347.

Son, YJ, Trachtenberg, JT, Thompson, WJ (1996) Schwann cells induce and guide sprouting and reinnervation of neuromuscular junctions. Trends Neurosci, 19:280–285.

Topilko, P, Levi, G, Merlo, G, Mantero, S, Desmarquet, C, Mancardi, G, Charnay, P (1997) Differential regulation of the zinc finger genes Krox-20 and Krox-24 (Egr-1) suggests antagonistic roles in Schwann cells. J Neurosci Res, 50:702–712.

Topilko, P, Schneider-Maunoury, S, Levi, G, Baron-Van Evercooren, A, Chennoufi, AB, Seitanidou, T, Babinet, C, Charnay, P (1994) Krox-20 controls myelination in the peripheral nervous system. Nature, 371(6500):796–799.

Woolf, CJ, Reynolds, ML, Chong, MS, Emson, P, Irwin, N, Benowitz, LI (1992) Denervation of the motor endplate results in the rapid expression by terminal Schwann cells of the growth-associated protein GAP-43. J Neurosci, 12:3999–4010.

Yang, XW, Wynder, C, Doughty, ML, Heintz, N (1999) BAC-mediated gene-dosage analysis reveals a role for Zipro1 (Ru49/Zfp38) in progenitor cell proliferation in cerebellum and skin. Nat Genet, 22:327–335.

Yang, XW, Zhong, R, Heintz, N (1996) Granule cell specification in the developing mouse brain as defined by expression of the zinc finger transcription factor RU49. Development, 122:555–566.

You, S, Petrov, T, Chung, PH, Gordon, T (1997) The expression of the low affinity nerve growth factor receptor in long-term denervated Schwann cells. Glia, 20:87–100.

Zuo, Y, Lubischer, JL, Kang, H, Tian, L, Mikesh, M, Marks, A, Scofield, VL, Maika, S, Newman, C, Krieg, P, Thompson, WJ (2004) Fluorescent proteins expressed in mouse transgenic lines mark subsets of glia, neurons, macrophages, and dendritic cells for vital

examination. J Neurosci, 24:10999–11009.

VITA

Elaine Louis Ellerton was born in Colchester, England on October 31st, 1973. She is the only daughter of Anneliese Marie-Hildegard (Lenz) and John Wyn Ellerton. After graduating from Torrey Pines High School in Del Mar, California, she attended MiraCosta College and then finished up her Bachelors of Science at the University of California at San Diego. She received a Bachelors of Science in general biology in 1998. She then worked as a research assistant at UCSD for a year before getting her Masters of Science degree from the California School of Professional Psychology. She worked for one year as a research associate at the Salk Institute and in 2003 she transferred into the Doctoral Program in Neuroscience at the University of Texas at Austin.

Permanent address: 5204 Avenue G, Austin, Texas, 78751.

This dissertation was typed by the author.